mathematics

MDPI

Article

On the Properties of a Newly Susceptible, Non-Seriously Infected, Hospitalized, and Recovered Subpopulation Epidemic Model

Carmen Legarreta *, Manuel De la Sen * and Santiago Alonso-Quesada

Department of Electricity and Electronics, Faculty of Science and Technology, University of the Basque Country, UPV/EHU, 48940 Leioa, Spain; santiago.alonso@ehu.eus

* Correspondence: carmen.legarreta@ehu.eus (C.L.); manuel.delasen@ehu.eus (M.D.l.S.)

Abstract: The COVID-19 outbreak has brought to the forefront the importance of predicting and controlling an epidemic outbreak with policies such as vaccination or reducing social contacts. This paper studies an SIHR epidemic model characterized by susceptible (S), non-seriously infected (I), hospitalized (H), and recovered (R) subpopulations, and dynamic vaccination; vaccination itself and H are fed back, and its dynamics are also determined by a free-design time-dependent function and parameters. From a theoretical analysis, the well-posedness of the model is demonstrated; positivity and the disease-free (P_{df}) and endemic (P_{ee}) equilibrium points are analyzed. The controlled reproduction number ($\mathcal{R}_c$) is proved to be a threshold for the local asymptotic stability of P_{df} and the existence P_{ee}; when $\mathcal{R}_c < 1$ ($\mathcal{R}_c > 1$), then P_{df} is (not) locally asymptotically stable and P_{ee} does not (does) exist. Simulations have been carried out with data concerning COVID-19 where the importance of keeping $\mathcal{R}_c < 1$ to prevent the disease spreading and future deaths is highlighted. We design the control input, since it can be easily adapted to match the user specification, to obtain impulsive and regular vaccination and fulfill the condition $\mathcal{R}_c < 1$.

Keywords: epidemiological model; SIHR model; COVID-19; feedback vaccination; regular vaccination; impulsive vaccination

MSC: 37N35; 34D23; 34D45; 34E10; 34H05; 92B05; 92D30

Citation: Legarreta, C.; De la Sen, M.; Alonso-Quesada, S. On the Properties of a Newly Susceptible, Non-Seriously Infected, Hospitalized, and Recovered Subpopulation Epidemic Model. *Mathematics* **2024**, *12*, 245. https://doi.org/10.3390/math12020245

Academic Editor: Dimplekumar N. Chalishajar

Received: 1 December 2023
Revised: 27 December 2023
Accepted: 1 January 2024
Published: 11 January 2024

1. Introduction

In December 2019, after the increment in pneumonia cases in Wuhan (China), the authorities ordered respiratory tests to be carried out to find out its origin. They discovered that the new rise in these cases was caused by a novel virus, which was coincident with severe acute respiratory syndrome coronavirus (SARS-CoV) and other mammal coronaviruses (especially bat and pangolin); their similarity was more than 70% and 95%, respectively [1–3]. Therefore, this new virus was named SARS-CoV-2 (more commonly known as COVID-19) and, in spite of being spotlighted due to the pneumonia cases, it had recently been found via survey that the most common symptoms were cough, fever, and weakness [4,5]. Even though many countries implemented prevention measurements to avoid the spread of COVID-19, by 9 March 2020, more than 118,000 cases and 4291 deaths were reported in 114 countries, and the World Health Organization (WHO) characterized this virus as a pandemic [6]. This situation highlighted the importance of epidemic models, and some derived terms such as the effective reproduction number or herd immunity, which allow the epidemic situation and its future behaviour to be determined.

The basic idea behind these mathematical models is to split the population into different subpopulations depending on their medical condition [7–15], so the SIR model (which divides the population into susceptible, infectious, and recovered subpopulations), SEIR model (the exposed subpopulation is included in the SIR model), etc. are built up,

and the conditions to eradicate the disease are usually obtained and analyzed. For example, in [14], the vaccination coverage level needed to eliminate Ebola from a population is given and, in [15], different prevention policies are compared. Usually, diseases do not affect different age groups homogeneously (i.e., the elderly population are often more sensitive to diseases), so many studies consider age-group epidemic models [16–19]. While the complexity is increased, the obtained results are more precise. For instance, in [16], data concerning the COVID-19 epidemic evolution in Shijiazhuang City, Hebei Province in China and three different prevention strategies, with respect to different age groups, are characterized by a set of epidemic features, which gives an overview of each strategy's impact. In [17], to reach the WHO's target measles incidence rate in India, they concluded that it is necessary to increase the vaccination coverage rate among children of age 0–4 years. The literature regarding control techniques for epidemic models is also exhaustive; in some studies, they apply constant and pulse vaccination [20–23], and they show it to be simple and effective. Other studies use control theory techniques, such as feedback control [24–26], and they show better convergence time and steady-state errors. Machine learning has also been applied to make more accurate models and therefore tackle more efficiently the control problem [27–31].

In addition, due to the global impact caused by COVID-19, many studies have put into practice this kind of mathematical model for this specific case; the works in [32,33] consider a quarantine subpopulation, and the condition that makes the disease disappear from the whole population is obtained. Moreover, in both cases, the model is validated with real data regarding the epidemic evolution in Saudi Arabia [32] and Italy [33], so its future evolution can be predicted. During the first stage of the COVID-19 epidemic evolution, as no vaccine was available, reducing social contact was a widely adopted measurement all over the world, and the impact of this prevention method is researched in [34,35]. Other works included vaccination strategies such as newborn vaccination [36], vaccinating a proportion of the susceptible subpopulation [37,38], and implementing dynamic vaccination and treatment with an SIR-like model [39]. All of these analyze the local and global stability of their respective systems' equilibrium points, among other things.

In this paper, an SIHR model has been built up where the total population has been divided into susceptible (S), non-seriously infected (I), hospitalized (H), and recovered (R) subpopulations, and a vaccination control strategy has been included. Thus, taking each subpopulation as a state variable and vaccination as the input variable, this model lays out a set of first-order non-linear differential equations. It has been assumed, as in a real-case situation, that S, I, and R are unknown, so only vaccination and hospitalized variables have been fed back to the vaccination dynamics through the gains c_1 and c_2, respectively. Moreover, to make a flexible vaccination, a free-design time-dependent function $f(t)$ has been included in the vaccination control dynamics. From the formulated system, the disease-free equilibrium point (P_{df}) and the endemic equilibrium point (P_{ee}) have been calculated, and it has been proved that P_{ee} is reachable under certain conditions. In addition, considering the existence of a vaccination and making the right choice of the free-design parameters (c_1, c_2, and c_3), it is possible to turn P_{ee} into P_{df}. The conditions for the global and local asymptotic stability of P_{df} have been obtained. In the case of the endemic equilibrium point in absence of vaccination (P_{ee}^{nv}), the Routh–Hurwitz criterion has been used to conclude that it is locally asymptotically stable whenever it is reachable and, from Rouche's theorem, the conditions for the local asymptotic stability of P_{ee} have been inferred.

Finally, a value has been given to each parameter based on the background literature [40–45], and several simulations have been carried out to reinforce and display the achieved theoretical results. Overall, the main novelties that this paper presents are as follows:

(i) The implementation of a vaccination (dynamic control input), where hospitalization and the vaccination itself are fed back;
(ii) Including a free-design time-dependent function into vaccination;

(iii) Considering the vaccine stock in the vaccination strategy;
(iv) A strategy to choose the vaccination free-design time-dependent function and parameters such that P_{df} and P_{ee} are locally asymptotically stable and unstable, respectively.

The first novelty, in comparison with the background literature, gives a more realistic feedback vaccination control; it includes only hospitalization and vaccination state variables as feedback of the vaccination dynamics, which are related to data that are usually known or accessible. This vaccination can easily be adapted to the desired specifications since it includes a free-design time-dependent function (second novelty). Meanwhile, in practice, the vaccines stockpile is reduced as they are provided; many epidemic models usually ignore this constrain. Therefore, the introduced vaccination has been constrained by the vaccines stockpile; the number of individuals who receive a dose cannot exceed the vaccines stock (third novelty). This characteristic, with the fact of free-design parameters (c_1, c_2, and c_3), allows a realistic vaccination strategy to be designed. The controlled reproduction number ($\mathcal{R}_c$), which depends on c_1 and c_3, has been found to be a fundamental part of the local asymptotic stability of P_{df} and its uniqueness. So, with the objective of reducing as much as possible the epidemic impact, one can consider $\mathcal{R}_c$ and select a pair of c_1 and c_3 to ensure the local asymptotic stability of P_{df} (fourth novelty). However, if the condition for the local asymptotic stability of P_{df} can not be accomplished (i.e., there is a low vaccine reserves), one can consider a suitable P_{ee} and the conditions that make it locally asymptotically stable.

The paper is organized as follows: Section 2 describes the SIHR model within the vaccination policy: what characterized the subpopulations, which parameters are taken into account, how vaccination affects each subpopulation, and how each subpopulation transforms into another. Thus, the resulting first-order non-linear differential system is formulated. Afterwards, considering non-negative initial conditions, the non-negativity of each state variable, with and without vaccination, is studied and proved. Finally, from the dynamical system, P_{df} and P_{ee} are obtained, and the conditions for their existence are discussed. Section 3 is divided into three subsections; Sections 3.1 and 3.2 are focused on the stability analysis of P_{df}, whereas Section 3.3 focuses on P_{ee}. In Section 3.1, the condition for the local asymptotic stability of P_{df} is proved with the next generation matrices and, in Section 3.2, the solutions of the differential equations are used to derive a sufficient condition for the global stability. In Section 3.3, the system is linearized about P_{ee}, and the Jacobian matrix is inferred. Then, the eigenvalue problem of the Jacobian matrix is formulated, and the conditions that ensure a negative real part for all eigenvalues (so P_{ee} is locally asymptotically stable) are obtained from the Routh–Hurwitz criterion and Rouche's theorem. In Section 4, several simulations have been carried out which show an accordance between the theoretical results and the numerical ones. Moreover, in a simulation where a vaccine stock function has been introduced, the free-design parameters and function have been chosen based on a desired vaccination strategy. In addition to illustrating the desired behavior, it shows that the disease is eradicated. Finally, the paper ends with Section 5, where the results are discussed.

2. Model Description

When diseases spread through big populations, in terms of prediction, deterministic models have been proven to give good results, so a deterministic model has been built up. This type of models is usually represented by flow charts, which are composed by two main parts: blocks and arrows. Each block stands for a subpopulation characterized by its medical condition (e.g., healthy, sick, recovered, etc.), while the arrows indicate how individuals from one block transform into another.

Figure 1 shows the deterministic system which adds a new block (H) to the SIR model. Those compartments are used to represents the following subpopulations:

- Susceptible (S): Group of individuals that can catch the disease. They are not yet infected nor have immunity against it.

- Non-seriously infected (I): Group of individuals that caught the disease and present symptoms. They are contagious and therefore responsible for the disease spreading. It is assumed that they do not have grave symptoms. Note that in order to simplify the technical nomenclature, the non-seriously infected population is simply referred to as the "infected subpopulation" in the sequel.
- Hospitalized (H): This group of people is characterized by suffering from serious symptoms and therefore being hospitalized. Since they are hospitalized, it is assumed that prevention measurements are strict, and consequently, they are not contagious.
- Recovered (R): Group of individuals with immunity on them, that is; infected or hospitalized people that already have been recovered or those susceptibles that were vaccinated.
- Vaccinated (v): It defines the number of susceptible people vaccinated per unit time which are introduced in the recovered subpopulation. It is used for control purposes.

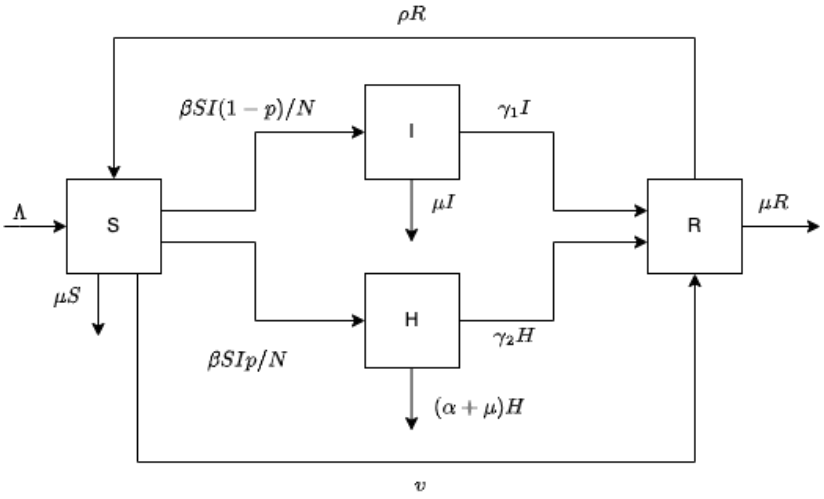

Figure 1. System flow chart.

The parameters appearing in Figure 1 are:

- Λ: newborns per unit time.
- β: transmission rate.
- μ: natural mortality rate.
- p: probability of being hospitalized once you catch the disease.
- γ_1: recovery rate of non-seriously infected individuals.
- γ_2: recovery rate of hospitalized individuals.
- α: death rate of hospitalized individuals.
- ρ: immunity loss rate.

These parameters are conditioned by

$$0 \leq \Lambda, \beta, \mu, \gamma_1, \gamma_2, \alpha, \rho \quad \text{and} \quad 0 \leq p \leq 1. \tag{1}$$

N is the total population size, and it is assumed to be sufficiently large. Newborns are incorporated to the class S with a rate Λ. Considering that all inhabitants die naturally indistinctly to the subpopulaiton they belong to, a portion proportional to μ will be removed from all compartments. Hospitalized individuals not only will die naturally but also due to the disease; a portion αH will also be removed.

Assuming that the population is homogeneously mixed, the rate β indicates the probability of infecting susceptible individuals when they are in contact with infected individuals. Thus, the mathematical expressions is

$$\beta = cp_i, \tag{2}$$

where c is the average number of close contacts per day of a member from I, and p_i is the probability of infecting susceptible individuals when there is a close contact. Hence, how the susceptible individuals get infected can be defined; there is a probability cI/N that an individual from S contacts an individual from I. Therefore, an individual from S has a probability $\beta I/N$ of being infected, and consequently, $\beta IS/N$ susceptible individuals will be infected. Models with this type of transmission are known as mass action models.

The probability of those who caught the disease being hospitalized is p, so $\beta ISp/N$ individuals will be hospitalized. The rest $(\beta IS(1-p)/N)$ will go to I. Infected individuals from I and H subpopulations will recover at rates γ_1 and γ_2, respectively; that is, $\gamma_1 I$ and $\gamma_2 H$ will be removed from I and H, respectively, and they will be introduced into R. The vaccinated susceptible individuals per day (v) are extracted from S and brought to R. However, immunity disappears after ρ^{-1} days, and they become susceptible again.

Each state variation with respect to time is equal to the added individuals minus the removed ones. Thus, the flow chart shown in Figure 1 leads to the following time differential system,

$$\begin{array}{rcl} \dot{S}(t) & = & \Lambda + \rho R(t) - \frac{\beta I(t)S(t)}{N(t)} - \mu S(t) - v(t), \\ \dot{I}(t) & = & \frac{\beta I(t)S(t)(1-p)}{N(t)} - (\mu + \gamma_1)I(t), \\ \dot{H}(t) & = & \frac{\beta I(t)S(t)p}{N(t)} - (\mu + \gamma_2 + \alpha)H(t), \\ \dot{R}(t) & = & \gamma_1 I(t) + \gamma_2 H(t) + v(t) - (\rho + \mu)R(t), \end{array} \tag{3}$$

and initial conditions $S(0) \geq 0$, $I(0) \geq 0$, $H(0) \geq 0$, and $R(0) \geq 0$. Regarding the total population,

$$\begin{array}{rcl} N(t) & = & S(t) + I(t) + H(t) + R(t), \\ \dot{N}(t) & = & \Lambda - \mu N(t) - \alpha H(t). \end{array} \tag{4}$$

The controller $v(t)$ is defined by the following equation:

$$\dot{v}(t) = -c_1 v(t) + c_2 H(t) + c_3 + f(t), \tag{5}$$

where $c_i \geq 0 \ : \ i \in \{1, 2, 3\}$ are tuning parameters adjusted to yield a desired behavior, and $f(t)$ represents the free-design time-dependent function. Note that Equation (5) is a first-order differential equation, where only $v(t)$ and $H(t)$ are taken into account, and its solution will be a feedback function of the state variables and time.

2.1. Non-Negativity of the Solution

To demonstrate the consistency of the equations given in (3), (4), and (5) the sizes of the subpopulations $S(t)$, $I(t)$, $H(t)$, and $R(t)$, and the total population $N(t)$ must be non-negative as well as the vaccination per unit time $v(t)$. It can be shown that all the solutions will be kept non-negative for a given finite non-negative initial condition under certain reasonable constrains.

Theorem 1. *Assuming that there is no vaccination ($v(t) = 0$ for all time), the following properties hold:*

(i) The solution of the epidemic model defined by the set of Equation (3) is non-negative for all $t > 0$ and for any finite initial condition such that $S(0) \geq 0$, $I(0) \geq 0$, $H(0) \geq 0$, and $R(0) \geq 0$.

(ii) The set

$$\mathbf{D} = \left\{ (S, I, H, R) \in \mathbb{R}^4_+ : N \leq \frac{\Lambda}{\mu} \right\}, \tag{6}$$

where $\mathbb{R}^4_+ = \{x \in \mathbb{R}^4 : x \geq 0\}$, is positively invariant with respect to the dynamical system (3).

Proof of Theorem 1. Since the differential equations shown in (3) and (4) are first-order differential equations, each solution is obtained with the superposition of the respective homogeneous part and the forcing part, so it leads to

$$\begin{aligned} S(t) &= S(0)e^{-\int_0^t \left(\mu+\frac{\beta I(\tau)}{N(\tau)}\right)d\tau} + \int_0^t e^{\int_0^{t-\tau}\left(\mu+\frac{\beta I(\tau')}{N(\tau')}\right)d\tau'}(\Lambda+\rho R(\tau))d\tau, \\ I(t) &= I(0)e^{-\int_0^t \left(\mu+\gamma_1-\frac{\beta S(\tau)(1-p)}{N(\tau)}\right)d\tau}, \\ H(t) &= H(0)e^{-(\mu+\gamma_2+\alpha)t} + \int_0^t e^{-(\mu+\gamma_2+\alpha)(t-\tau)}\left(\frac{\beta I(\tau)S(\tau)p}{N(\tau)}\right)d\tau, \\ R(t) &= R(0)e^{-(\rho+\mu)t} + \int_0^t e^{-(\rho+\mu)(t-\tau)}(\gamma_1 I(\tau)+\gamma_2 H(\tau))d\tau. \end{aligned} \tag{7}$$

From (7), it is straightforward that $I(t)$ is non-negative for all time if the initial condition is non-negative. By introducing the expressions for $I(t)$ and $H(t)$ into $R(t)$, one obtains:

$$\begin{aligned} R(t) &= R(0)e^{-(\rho+\mu)t} + \int_0^t e^{-(\rho+\mu)(t-\tau)}\left(\gamma_1\left[I(0)e^{-\int_0^\tau\left(\mu+\gamma_1-\frac{\beta S(\tau')(1-p)}{N(\tau')}\right)d\tau'}\right]\right. \\ &+ \left.\gamma_2\left[H(0)e^{-(\mu+\gamma_2+\alpha)\tau} + \int_0^\tau e^{-(\mu+\gamma_2+\alpha)(\tau-\tau')}\left(\frac{\beta I(\tau')S(\tau')p}{N(\tau')}\right)d\tau'\right]\right)d\tau. \end{aligned} \tag{8}$$

From (7) and (8), it follows that:

$$\begin{aligned} S(t) &= S(0)e^{-\int_0^t\left(\mu+\frac{\beta I(\tau)}{N(\tau)}\right)d\tau} + \int_0^t e^{\int_0^{t-\tau}\left(\mu+\frac{\beta I(\tau')}{N(\tau')}\right)d\tau'}\left(\Lambda+\rho\left\{R(0)e^{-(\rho+\mu)\tau}\right.\right. \\ &+ \int_0^\tau e^{-(\rho+\mu)(\tau-\tau')}\left(\gamma_1\left[I(0)e^{-\int_0^{\tau'}\left(\mu+\gamma_1-\frac{\beta S(\tau'')(1-p)}{N(\tau'')}\right)d\tau''}\right]\right. \\ &+ \left.\left.\left.\gamma_2\left[H(0)e^{-(\mu+\gamma_2+\alpha)\tau'} + \int_0^{\tau'} e^{-(\mu+\gamma_2+\alpha)(\tau'-\tau'')}\left(\frac{\beta I(\tau'')S(\tau'')}{N(\tau'')}\right)d\tau''\right]\right)d\tau'\right\}\right)d\tau. \end{aligned} \tag{9}$$

After removing some terms from (9), the next inequality can be obtained:

$$S(t) \geq \overline{S(t)} = \rho\gamma_2\int_0^t e^{\int_0^{t-\tau}\left(\mu+\frac{\beta I(\tau')}{N(\tau')}\right)d\tau'}\int_0^\tau e^{-(\rho+\mu)(\tau-\tau')}\int_0^{\tau'} e^{-(\mu+\gamma_2+\alpha)(\tau'-\tau'')}\left(\frac{\beta I(\tau'')S(\tau'')}{N(\tau'')}\right)d\tau''d\tau'd\tau. \tag{10}$$

From the expression above, it follows that $\overline{S(t)} \geq 0 \implies S(t) \geq 0$. Therefore, we proceed by contradiction to prove that $\overline{S(t)} \geq 0$. Assume that t_1 is the first time instant at which $\overline{S(t_1)} < 0$. Taking into account that $I(t) \geq 0$ for all $t \in [0, \infty)$ since $I(0) \geq 0$, see the second equation in (3), the condition $\overline{S(t_1)} < 0$ can only be fulfilled if the total population was negative in a previous time interval. Therefore, it will be assumed that there exists a time interval at which the total population becomes negative; that is, $N(t) \geq 0$ for any $t \in [0, t_2]$, and $N(t) < 0$ for any $t \in (t_2, t_1)$.

From the expression for $H(t)$ in (7), it is concluded that $H(t) \geq 0$ for $t \in [0, t_2]$ as a result of $\beta I(\tau)S(\tau)/N(\tau)$ non-negativeness, since $S(t)$, $I(t)$, and $N(t)$ are non-negative during the given time interval. As all the integrands of $R(t)$ are non-negative, see (7), $R(t)$ will also be non-negative.

Now, considering the time derivative of $N(t)$ given in (4), its solution is obtained by direct calculation:

$$N(t) = N(0)e^{-\mu t} + \int_0^t e^{-\mu(t-\tau)}(\Lambda - \alpha H(\tau))d\tau, \tag{11}$$

and, by substituting the expression for $H(t)$ in (7) into (11), it follows that:

$$N(t) = N(0)e^{-\mu t} + \int_0^t e^{-\mu(t-\tau)}\left(\Lambda - \alpha\left[H(0)e^{-(\mu+\gamma_2+\alpha)\tau} + \int_0^\tau e^{-(\mu+\gamma_2+\alpha)(\tau-\tau')}\left(\frac{\beta I(\tau')S(\tau')p}{N(\tau')}\right)d\tau'\right]\right)d\tau. \tag{12}$$

Let $\tilde{N}(t, t_0)$ be defined as

$$\tilde{N}(t,t_0) = N(t_0)e^{-\mu(t-t_0)} + \int_{t_0}^{t} e^{-\mu(t-\tau)}\Big(\Lambda - \alpha H(t_0)e^{-(\mu+\gamma_2+\alpha)\tau}\Big)d\tau, \tag{13}$$

and it yields

$$\tilde{N}(t,t_0) = e^{-\mu(t-t_0)}\left(N(t_0) - \frac{\alpha H(t_0)}{\gamma_2+\alpha}\right) + \frac{\Lambda}{\mu}\Big(1 - e^{-\mu(t-t_0)}\Big) + \frac{\alpha H(t_0)}{\gamma_2+\alpha}e^{-(\mu+\gamma_2+\alpha)(t-t_0)}. \tag{14}$$

Taking into account that $N(t_0) = S(t_0) + I(t_0) + H(t_0) + R(t_0)$, it leads to

$$\tilde{N}(t,t_0) = e^{-\mu(t-t_0)}\left[S(t_0) + I(t_0) + H(t_0)\left(1 - \frac{\alpha}{\gamma_2+\alpha}\right) + R(t_0)\right] + \frac{\Lambda}{\mu}\Big(1 - e^{-\mu(t-t_0)}\Big) + \frac{\alpha H(t_0)}{\gamma_2+\alpha}e^{-(\mu+\gamma_2+\alpha)(t-t_0)}. \tag{15}$$

Previously, it was found that all the subpopulations are non-negative for any $t \in [0, t_2]$. Therefore, it follows that $\tilde{N}(t,t_0) \geq 0$ for any $t_0 \in [0,t_2]$ and $t \in [0,\infty)$, where $t_0 \leq t$. Continuing with the contradiction, for any $t \in (t_2, t_1)$, Equation (12) can be rewritten as follows:

$$N(t) = \tilde{N}(t,t_2) + \alpha\left(\int_{t_2}^{t} e^{-\mu(t-\tau)}\int_{t_2}^{\tau} e^{-(\mu+\gamma_2+\alpha)(\tau-\tau')}\left(\frac{\beta I(\tau')S(\tau')p}{|N(\tau')|}\right)d\tau' d\tau\right) \geq 0, \tag{16}$$

which contradicts the existence of a time interval where $N(t) < 0$. Therefore, $N(t) \geq 0$ for all $t \in [0,\infty)$, and consequently, a t_1 at which $\overline{S(t_1)} < 0$ does not exist. Thus, from (10), one concludes that $\overline{S(t)} \geq 0$, and $S(t) \geq 0$ too, for all $t \in [0,\infty)$. It was previously proved that $I(t)$, $S(t)$, and $N(t)$ non-negativity implies $H(t)$ and $R(t)$ non-negativity, so property (*i*) is proved.

Moreover, considering that nobody is dying because of the disease ($\alpha = 0$), it is possible to prove that the entire population will be bounded. The solution of the differential Equation (4) is given by

$$N(t) = \left(N(0) - \frac{\Lambda}{\mu}\right)e^{-\mu t} + \frac{\Lambda}{\mu}, \tag{17}$$

and the limit

$$\lim_{t\to\infty}\left[\left(N(0) - \frac{\Lambda}{\mu}\right)e^{-\mu t} + \frac{\Lambda}{\mu}\right] = \frac{\Lambda}{\mu}. \tag{18}$$

So, let **D** be a set defined as

$$\mathbf{D} = \left\{(S,I,H,R) \in \mathbb{R}^4_+ : N \leq \frac{\Lambda}{\mu}\right\}, \tag{19}$$

where $\mathbb{R}^4_+ = \{x \in \mathbb{R}^4 : x \geq 0\}$. Hence, given any initial condition belonging to **D**, the solution of system (3) will remain in **D**. Therefore, the set **D** is positively invariant and Property (ii) is proved. □

Theorem 2. *If a vaccination $v(t)$ exists, the following properties hold:*

(i) The solution of the epidemic model, defined by the set of equations in (3) and (5), is non-negative for any initial condition such that $S(0) \geq 0$, $I(0) \geq 0$, $H(0) \geq 0$, $R(0) \geq 0$, and $v(0) \geq 0$, if the following condition is accomplished:

$$\max\left(0, f_{Im}(t)\right) \leq f_I(t) \leq f_{IM}(t), \tag{20}$$

where $f_I(t)$, $f_{Im}(t)$, and $f_{IM}(t)$ are defined as follows:

$$\begin{aligned}
\dot{f}_I(t) &= f(t),\\
f_{Im}(t) &= -v(0)e^{-c_1 t} - c_2\int_0^t e^{-c_1(t-\tau)}H(\tau)d\tau - \tfrac{c_3}{c_1}\left(1-e^{-c_1 t}\right) + f_I(0)e^{-c_1 t} + c_1\int_0^t e^{-c_1(t-\tau)}f_I(\tau)d\tau, \quad \textit{and}\\
f_{IM}(t) &= min(\overline{v(t)}, v_s(t)) - v(0)e^{-c_1 t} - c_2\int_0^t e^{-c_1(t-\tau)}H(\tau)d\tau - \tfrac{c_3}{c_1}\left(1-e^{-c_1 t}\right) + f_I(0)e^{-c_1 t} + c_1\int_0^t e^{-c_1(t-\tau)}f_I(\tau)d\tau.
\end{aligned}$$

$\overline{v(t)}$ and $v_s(t)$ are the maximum number of susceptible individuals that can be vaccinated and the vaccination stock, respectively, where $0 \leq v_s(t)$, and

$$\overline{v(t)} = S(t) + \Lambda + \rho R(t). \tag{21}$$

(ii) The set **D** *is positively invariant with respect to the dynamical system (3).*

Proof of Theorem 2. First, the solution of $v(t)$ is calculated:

$$v(t) = v(0)e^{-c_1 t} + c_2\int_0^t e^{-c_1(t-\tau)}H(\tau)d\tau + \frac{c_3}{c_1}\left(1-e^{-c_1 t}\right) + \int_0^t e^{-c_1(t-\tau)}f(\tau)d\tau. \tag{22}$$

Considering that $f(t) = \dot{f}_I(t)$ and substituting into (22), one obtains:

$$v(t) = v(0)e^{-c_1 t} + c_2\int_0^t e^{-c_1(t-\tau)}H(\tau)d\tau + \frac{c_3}{c_1}\left(1-e^{-c_1 t}\right) + \int_0^t e^{-c_1(t-\tau)}\dot{f}_I(\tau)d\tau, \tag{23}$$

and, by applying the integration by parts, it follows that:

$$v(t) = v(0)e^{-c_1 t} + c_2\int_0^t e^{-c_1(t-\tau)}H(\tau)d\tau + \frac{c_3}{c_1}\left(1-e^{-c_1 t}\right) + f_I(t) - f_I(0)e^{-c_1 t} - c_1\int_0^t e^{-c_1(t-\tau)}f_I(\tau)d\tau \tag{24}$$

so the expression for $f_I(t)$ is

$$f_I(t) = v(t) - v(0)e^{-c_1 t} - c_2\int_0^t e^{-c_1(t-\tau)}H(\tau)d\tau - \frac{c_3}{c_1}\left(1-e^{-c_1 t}\right) + f_I(0)e^{-c_1 t} + c_1\int_0^t e^{-c_1(t-\tau)}f_I(\tau)d\tau. \tag{25}$$

Depending on the non-negativity of f_{Im}, two possibilities are found; if $f_{Im} \geq 0$, then $f_{Im} \leq f_I$ is necessary so that $v(t) \geq 0$. In contrast, if $f_{Im} < 0$, then $f_I = 0$ is sufficient so that $v(t) \geq 0$. Therefore, if the left part inequality in (20) is accomplished, $0 \leq v(t)$ is proved to be true. If the right part inequality in (20) is fulfilled, then $v(t) \leq \min(\overline{v(t)}, v_s(t))$. Then, $0 \leq \min\left(\overline{v(t)}, v_s(t)\right)$ provided that (20) is fulfilled.

To prove each subpopulation's non-negativity through time, the solutions of the equations shown in (3) have been calculated:

$$\begin{aligned}
S(t) &= S(0)e^{-\int_0^t\left(\mu+\frac{\beta I(\tau)}{N(\tau)}\right)d\tau} + \int_0^t e^{\int_0^{t-\tau}\left(\mu+\frac{\beta I(\tau')}{N(\tau')}\right)d\tau'}(\Lambda + \rho R(\tau) - v(\tau))d\tau,\\
I(t) &= I(0)e^{-\int_0^t\left(\mu+\gamma_1-\frac{\beta S(\tau)(1-p)}{N(\tau)}\right)d\tau},\\
H(t) &= H(0)e^{-(\mu+\gamma_2+\alpha)t} + \int_0^t e^{-(\mu+\gamma_2+\alpha)(t-\tau)}\left(\frac{\beta I(\tau)S(\tau)p}{N(\tau)}\right)d\tau,\\
R(t) &= R(0)e^{-(\rho+\mu)t} + \int_0^t e^{-(\rho+\mu)(t-\tau)}(\gamma_1 I(\tau) + \gamma_2 H(\tau) + v(\tau))d\tau.
\end{aligned} \tag{26}$$

Taking into account the solution of $S(t)$ given in (26), and the constrain $v(t) \leq \overline{v(t)}$, it leads to

$$S(t) \geq \overline{S(t)} = S(0)e^{-\int_0^t\left(\mu+\frac{\beta I(\tau)}{N(\tau)}\right)d\tau} - \int_0^t e^{\int_0^{t-\tau}\left(\mu+\frac{\beta I(\tau')}{N(\tau')}\right)d\tau'}S(\tau)d\tau. \tag{27}$$

By contradiction, it will be demonstrated that $S(t)$ is positive for all $t \in [0, \infty)$ and $S(0) \geq 0$. Let us suppose that $\overline{S(t)}$ becomes negative during a time interval; that is, $S(t) \geq 0$ for any $t \in [0, t_1)$, and $S(t) < 0$ for any $t \in (t_1, t_2)$. Then,

$$\overline{S(t)} \geq S(t_1) e^{-\int_{t_1}^{t} \left(\mu + \frac{\beta I(\tau)}{N(\tau)}\right) d\tau} + \int_{t_1}^{t} e^{\int_{0}^{t-\tau} \left(\mu + \frac{\beta I(\tau')}{N(\tau')}\right) d\tau'} |S(\tau)| d\tau \geq 0. \tag{28}$$

Thus, a time interval at which $\overline{S(t)} < 0$ does not exist, so $\overline{S(t)} \geq 0 \implies S(t) \geq 0$ for all $t \in [0, \infty)$.

Now, as in the proof of Theorem 1, we proceed by contradiction to conclude that $N(t) \geq 0$ for all $t \in [0, \infty)$; let us assume that $N(t) \geq 0$ for any $t \in [0, t_1]$, and $N(t) < 0$ for any $t \in (t_1, t_2)$, then $H(t) \geq 0$ for $t \in [0, t_1]$ since $\beta I(\tau) S(\tau) / N(\tau)$ is non-negative during $t \in [0, t_1]$. From the solution of $R(t)$ given in (26), it follows that $R(t) \geq 0$ for any $t \in [0, t_1]$ as all the integrands are non-negative. Regarding the solution of $N(t)$, the expression given in (12) is still valid for the system (3) when vaccination is being applied, and $\tilde{N}(t, t_1) \geq 0$ for all $t > t_1$ since all the subpopulations are non-negative at t_1. Thus,

$$N(t) = \tilde{N}(t, t_1) + \alpha \left(\int_{t_1}^{t} e^{-\mu(t-\tau)} \int_{t_1}^{\tau} e^{-(\mu+\gamma_2+\alpha)(\tau-\tau')} \left(\frac{\beta I(\tau') S(\tau') p}{|N(\tau')|} \right) d\tau' d\tau \right) \geq 0, \tag{29}$$

so a time interval (t_1, t_2) where $N(t) < 0$ does not exist, and consequently, $N(t) \geq 0$ for all $t \in [0, \infty)$. Property (i) is proved.

Considering that nobody dies due to the disease, the solution of the differential Equation (4) is given by the expression (17). Consequently, the set $\mathbf{D}$, see (19), is positively invariant with respect to the dynamical system (3) with vaccination. Property (ii) is proved. □

2.2. Equilibrium Points

At an equilibrium point, the system variables do not change with respect to time; therefore, the time derivatives in (3) and (5) are set to zero ($\dot{S}(t) = \dot{I}(t) = \dot{H}(t) = \dot{R}(t) = \dot{v}(t) = 0$), and its solution will give the equilibrium points. Two different equilibrium points are found: P_{df} and P_{ee}.

Definition 1. *P_{df} is an equilibrium point of the system (3), and it is characterized by a null infected subpopulation:*

$$P_{df} = (S_{df}, I_{df}, H_{df}, R_{df}, v_{df}), \tag{30}$$

where

$$\begin{array}{lllllll} S_{df} & = & \frac{\Lambda}{\mu} - \frac{c_3+f}{c_1(\rho+\mu)}, & I_{df} & = & 0, & H_{df} = 0, \\ R_{df} & = & \frac{c_3+f}{c_1(\rho+\mu)}, & v_{df} & = & \frac{c_3+f}{c_1}, & \end{array} \tag{31}$$

and the total population $N_{df} = \Lambda / \mu$.

This result shows that the susceptible and the recovered subpopulations hold the whole population, and a population exchange exists between them due to vaccination. Moreover, vaccination effort must be limited to not contradict Theorem 2 and consequently ensure the solution's non-negativeness. In a real situation, this implies that it is not possible to vaccinate more individuals than those in the susceptible suppopulation.

Note that $f(t)$ has been considered as time-invariant ($f(t) \to f$) in order to calculate the equilibrium points.

Proposition 1. *P_{df} is reachable (each subpopulation has a non-negative value) if and only if the vaccination control law tuning parameters c_1 and c_3, and f, are chosen such that:*

$$0 \leq B \leq B_{df} = \frac{\Lambda(\rho + \mu)}{\mu}. \tag{32}$$

where $B = (c_3 + f)/c_1$.

Taking into account the expressions for each subpopulation given in (31), P_{df}^{nv} is defined as follows:

$$P_{df}^{nv} = (S_{df}^{nv}, I_{df}^{nv}, H_{df}^{nv}, R_{df}^{nv}, v_{df}^{nv}), \tag{33}$$

where

$$S_{df}^{nv} = \frac{\Lambda}{\mu}, \quad I_{df}^{nv} = 0, \quad H_{df}^{nv} = 0, \quad R_{df}^{nv} = 0, \quad v_{df}^{nv} = 0, \tag{34}$$

and, in this particular case, it can be observed that the S_{df}^{nv} holds the whole population: $N_{df}^{nv} = S_{df}^{nv}$.

Definition 2. *P_{ee} is an equilibrium point of the system (3), and it is characterized by a non-zero infected subpopulations ($I_{ee} > 0$ and $H_{ee} > 0$):*

$$P_{ee} = (S_{ee}, I_{ee}, H_{ee}, R_{ee}, v_{ee}), \tag{35}$$

where

$$\begin{array}{rclcrcl} S_{ee} & = & (\Lambda - \alpha H_{ee})\left(\frac{k_1}{\mu k_4}\right), & & I_{ee} & = & \frac{k_2(1-p)}{k_1 p} H_{ee}, \\ H_{ee} & = & \frac{(\Lambda k_3(k_1-k_4)+\mu k_4 B)pk_1}{k_5+k_6-A\mu k_4 pk_1}, & & R_{ee} & = & \frac{1}{k_3}\left[\left(\frac{(1-p)\gamma_1 k_2+p\gamma_2 k_1}{pk_1} + A\right)H_{ee} + B\right], \\ v_{ee} & = & AH_{ee} + B, & & & & \end{array} \tag{36}$$

and

$$\begin{array}{rclcrcl} k_1 & = & \mu + \gamma_1, & & k_2 & = & \mu + \gamma_2 + \alpha, \\ k_3 & = & \rho + \mu, & & k_4 & = & \beta(1-p), \\ k_5 & = & k_3 k_1 (p\alpha k_1 - k_4 k_2), & & k_6 & = & k_4 \rho((1-p)\gamma_1 k_2 + p\gamma_2 k_1), \\ A & = & \frac{c_2}{c_1}. & & & & \end{array} \tag{37}$$

The total population $N_{ee} = (\Lambda - \alpha H_{ee})\frac{1}{\mu}$.

Remark 1. *Considering Theorem 2 and all the subpopulations in (36), the following hold:*

(i) From the expression for S_{ee} in (36), it can be seen that a portion of the susceptible subpopulation, which is proportional to αH_{ee} (deaths due to the disease), is removed from S_{ee}. In the case of a disease with a high death rate, the number of deaths could surpass the newborns, and it could cause a negative value of S_{ee}, which contradicts Theorem 2.

(ii) Other variables' non-negativeness only depends on H_{ee}'s non-negativeness; that is, the variables I_{ee}, R_{ee} and v_{ee} are linear with respect to H_{ee}, and their respective independent parameters are positive, so the condition $H_{ee} > 0$ is sufficient to ensure $I_{ee} > 0$, $R_{ee} > 0$, and $v_{ee} > 0$.

(iii) Let $\Lambda k_3(k_1 - k_4) + \mu k_4 B \to 0$, then $P_{ee} \to P_{df}$; when $\Lambda k_3(k_1 - k_4) + \mu k_4 B \to 0$, then $H_{ee} \to 0$, $I_{ee} \to 0$, and $R_{ee} \to R_{df}$. Considering that $k_1/k_4 \to 1 - B\mu/(\Lambda k_3)$ (equivalent to $\Lambda k_3(k_1 - k_4) + \mu k_4 B \to 0$), it follows that $S_{ee} \to S_{df}$.

(iv) From the point above, it is possible to transform P_{ee} into P_{df} with a suitable vaccination; that is, B can be modified to $\Lambda k_3(k_1 - k_4) + \mu k_4 B \to 0$, or equivalently $\Lambda(\rho + \mu)(\gamma_1 + \mu - \beta(1-p)) + \mu\beta(1-p)\frac{c_3+f}{c_1} \to 0$, so $P_{ee} \to P_{df}$.

Proposition 2. *The endemic equilibrium point is not reachable, in the sense that it has some negative component, if*

$$\beta(1-p) \leq \gamma_1 + \mu. \tag{38}$$

Proof of Proposition 2. Considering the expressions for S_{ee} and N_{ee} in (36), the normalized variable $s_{ee} = S_{ee}/N_{ee}$ is calculated:

$$s_{ee} = \frac{k_1}{k_4}. \tag{39}$$

If the condition $k_1 > k_4$ is fulfilled (i.e., $\gamma_1 + \mu > \beta(1-p)$), then $s_{ee} > 1$. This result contradicts Theorem 2 since it demonstrates that all the subpopulations are positive, and therefore all of them will be bounded by the whole population N; that is, the normalized subpopulation can not exceed 1.

If $k_1 = k_4$, then $s_{ee} = 1$, which implies that the susceptible subpopulation holds the whole population (i.e., $I_{ee} = H_{ee} = R_{ee} = 0$). This particular case does not correspond with the definition of P_{ee}, see Definition 2, but with the definition of P_{df}, see Definition 1. □

Proposition 3. *Assuming that:*

$$\beta(1-p) > \gamma_1 + \mu, \tag{40}$$

the endemic equilibrium point is reachable if the following conditions are fulfilled:

(i) $\frac{\beta(1-p)}{\gamma_1+\mu}\left(1 - \frac{\mu(c_3+f)}{c_1(\rho+\mu)\Lambda}\right) > 1$

(ii) $0 < c_1 < \infty$

Proof of Proposition 3. Considering the expression for the denominator of H_{ee} in (36):

$$d_H = k_5 + k_6 - A\mu k_4 p k_1, \tag{41}$$

and taking into account k_5 and k_6, by direct calculations, it is obtained that:

$$d_H = p\alpha k_1^2 k_3 - k_4\mu k_1 k_2 - k4\rho[p\gamma_1(\alpha+\mu) + (1-p)\gamma_2\mu + \mu(\alpha+\mu)] - A\mu k_4 p k_1. \tag{42}$$

Assuming that $k_4 > k_1$, it follows that:

$$d_H < k_3 k_1 p\alpha k_4 - k_4\mu k_1 k_2 - k_4\rho[p\gamma_1(\alpha+\mu) + (1-p)\gamma_2\mu + \mu(\alpha+\mu)] - A\mu k_4 p k_1, \tag{43}$$

which leads to

$$d_H < -k_4\mu\{[p\gamma_1 + (1-p)\gamma_2 + (1-p)\alpha + \mu]\rho + [(1-p)\alpha + \gamma_2 + \mu]k_1\} - A\mu k_4 p k_1 < 0. \tag{44}$$

If the condition (i) from Proposition 3 is fulfilled, the nominator of H_{ee} will be negative, and consequently, H_{ee} will be positive since its denominator is negative. □

Remark 2. *As it was mentioned in Remark 1, part (i), S_{ee} could reach a negative value due to a very aggressive disease. Taking into account the expression for S_{ee} in (36), it is concluded that this situation cannot occur if $\alpha H_{ee} < \Lambda$. By doing this, one obtains the following:*

$$\alpha p k_1(\Lambda k_3(k_4 - k_1) - \mu k_4 B) < -\Lambda d_H, \tag{45}$$

and considering expression (41), it follows that the inequality above is still true if the next inequality is fulfilled:

$$\alpha p\Lambda k_1 k_3(k_4 - k_1) < \Lambda\{-k_3 k_1 p\alpha k_1 + k_4\mu k_1 k_2 + k4\rho[p\gamma_1(\alpha+\mu) + (1-p)\gamma_2\mu + \mu(\alpha+\mu)] + A\mu k_4 p k_1\} \tag{46}$$

which leads to

$$0 < \Lambda\{k_4 k_1\mu(\alpha(1-p) + \gamma_2 + \mu) + k_4\rho[\gamma_1 p\mu(1-p)\gamma_2\mu + \mu((1-p)\alpha + \mu)]\}. \tag{47}$$

The condition above is always fulfilled, so a value of α that neglects the existence of S_{ee} does not exist.

The expressions for each subpopulation given in (36) include the particular case in which no vaccination is being applied. Thus, considering the expressions in (36), one can define P_{ee}^{nv} as follows:

$$P_{ee}^{nv} = (S_{ee}^{nv}, I_{ee}^{nv}, H_{ee}^{nv}, R_{ee}^{nv}, v_{ee}^{nv}), \tag{48}$$

where

$$\begin{array}{rclrclrcl} S_{ee}^{nv} & = & (\Lambda - \alpha H_{ee})\left(\frac{k_1}{\mu k_4}\right), & I_{ee}^{nv} & = & \frac{k_2(1-p)}{k_1 p} H_{ee}^{nv}, & H_{ee}^{nv} & = & \frac{\Lambda p k_1 k_3 (k_1 - k_4)}{k_5 + k_6}, \\ R_{ee}^{nv} & = & \left(\frac{(1-p)\gamma_1 k_2 + p\gamma_2 k_1}{p k_1 k_3}\right) H_{ee}, & v_{ee}^{nv} & = & 0, & & & \end{array} \tag{49}$$

and the total population $N_{ee}^{nv} = (\Lambda - \alpha H_{ee}^{nv})\frac{1}{\mu}$.

3. Stability of the Equilibrium Points

3.1. Local Stability of the Disease-Free Equilibrium Point

The basic reproduction number ($\mathcal{R}_0$) is a well-known parameter in epidemic models; it determines the number of secondary infections caused by an infected person when introduced to a disease-free equilibrium state type population without vaccination. Depending on its value, it is possible to determine whether the P_{df}^{nv} is locally asymptotically stable or not; that is, when its value is less than one ($\mathcal{R}_0 < 1$), P_{df}^{nv} is locally asymptotically stable. In contrast, if its value is greater than one ($\mathcal{R}_0 > 1$), P_{df}^{nv} is unstable. To obtain the mathematical expression for $\mathcal{R}_0$, the next generation matrices [7,46], $\mathcal{F}$ and $\mathcal{V}$, are used. The same procedure can be used to calculate $\mathcal{R}_c$; it is equivalent to $\mathcal{R}_0$ but taking into account the implemented vaccination.

$\mathcal{F}$ is defined as the rate of appearance of new infections in the subpopulations I and H, and $\mathcal{V}$ represents the transfer of individuals. Thus,

$$\mathcal{F} = \begin{pmatrix} \frac{\beta I(t) S(t)(1-p)}{N(t)} \\ \frac{\beta I(t) S(t) p}{N(t)} \end{pmatrix}, \qquad \mathcal{V} = \begin{pmatrix} (\mu + \gamma_1) I(t) \\ (\mu + \gamma_2 + \alpha) H(t) \end{pmatrix}. \tag{50}$$

The derivatives of $\mathcal{F}$ and $\mathcal{V}$ with respect to the vector $x(t) = (I(t)\ H(t))$, and evaluated at P_{df}, give the matrices F and V, respectively. Then,

$$F = \begin{pmatrix} \frac{\beta(1-p)S(t)(N(t)-I(t))}{N(t)^2} & 0 \\ \frac{\beta p S(t)(N(t)-I(t))}{N(t)^2} & 0 \end{pmatrix}\Bigg|_{P_{df}} = \begin{pmatrix} k_4\left(1 - \frac{\mu B}{k_3 \Lambda}\right) & 0 \\ (\beta - k_4)\left(1 - \frac{\mu B}{k_3 \Lambda}\right) & 0 \end{pmatrix}, \tag{51}$$

$$V = \begin{pmatrix} (\mu + \gamma_1) & 0 \\ 0 & (\mu + \gamma_2 + \alpha) \end{pmatrix}\Bigg|_{P_{df}} = \begin{pmatrix} k_1 & 0 \\ 0 & k_2 \end{pmatrix}. \tag{52}$$

Considering the expressions (51) and (52), $V^{-1}F$ is calculated

$$V^{-1}F = \begin{pmatrix} k_1^{-1} & 0 \\ 0 & k_2^{-1} \end{pmatrix} \begin{pmatrix} k_4\left(1 - \frac{\mu B}{k_3 \Lambda}\right) & 0 \\ (\beta - k_4)\left(1 - \frac{\mu B}{k_3 \Lambda}\right) & 0 \end{pmatrix} = \begin{pmatrix} \frac{k_4}{k_1}\left(1 - \frac{\mu B}{k_3 \Lambda}\right) & 0 \\ \left(\frac{\beta - k_4}{k_2}\right)\left(1 - \frac{\mu B}{k_3 \Lambda}\right) & 0 \end{pmatrix}, \tag{53}$$

and its spectral radius (the maximum of the absolute value of the eigenvalues) is equal to the basic reproduction number. From (53), it follows that:

$$\mathcal{R}_c = \sigma(V^{-1}F) = \frac{k_4}{k_1}\left(1 - \frac{\mu B}{k_3 \Lambda}\right) = \frac{\beta(1-p)}{\gamma_1 + \mu}\left(1 - \frac{\mu B}{(\rho + \mu)\Lambda}\right). \tag{54}$$

Theorem 3. *Assume that P_{df} is reachable. Then, it is locally asymptotically stable if and only if the control parameters are chosen such that:*

$$\mathcal{R}_c = \frac{\beta(1-p)}{\gamma_1 + \mu}\left(1 - \frac{\mu(c_3 + f)}{c_1(\rho + \mu)\Lambda}\right) < 1 \tag{55}$$

Proof of Theorem 3. If the eigenvalues of a linear system $\dot{\mathbf{x}}(t) = \mathbf{A}\mathbf{x}(t)$ have a negative real part, then the system is asymptotically stable. In case the system is non-linear, the

local asymptotic stability of the system about an equilibrium point $\mathbf{x}^*$ is determined by the eigenvalues of the system's Jacobian matrix $\mathbf{J}$ evaluated at the equilibrium point $\mathbf{x}^*$,

$$\mathbf{J} = \frac{d\mathbf{A}}{d\mathbf{x}}\Big|_{\mathbf{x}^*}. \tag{56}$$

If the eigenvalues of $\mathbf{J}$ have a negative real part, the system is locally asymptotically stable at the given equilibrium point $\mathbf{x}^*$.

Considering the systems (3) and (5), its Jacobian matrix gives

$$\mathbf{J} = \begin{pmatrix} -\frac{\beta I(N-S)}{N^2} - \mu & -\frac{\beta S(N-I)}{N^2} & \frac{\beta SI}{N^2} & \frac{\beta SI}{N^2} + \rho & -1 \\ \frac{k_4 I(N-S)}{N^2} & \frac{k_4 S(N-I)}{N^2} - k_1 & -\frac{k_4 SI}{N^2} & -\frac{k_4(1-p)SI}{N^2} & 0 \\ \frac{\beta pI(N-S)}{N^2} & \frac{\beta pS(N-I)}{N^2} & -\frac{\beta pSI}{N^2} - k_2 & -\frac{\beta pSI}{N^2} & 0 \\ 0 & \gamma_1 & \gamma_2 & -k_3 & 1 \\ 0 & 0 & c_2 & 0 & -c_1 \end{pmatrix}. \tag{57}$$

Evaluating the expression above at point P_{df} in (30), one obtains:

$$\mathbf{J} = \begin{pmatrix} -\mu & -\beta\left(1 - \frac{\mu B}{\Lambda k_3}\right) & 0 & \rho & -1 \\ 0 & k_4\left(1 - \frac{\mu B}{\Lambda k_3}\right) - k_1 & 0 & 0 & 0 \\ 0 & \beta\left(1 - \frac{\mu B}{\Lambda k_3}\right)p & -k_2 & 0 & 0 \\ 0 & \gamma_1 & \gamma_2 & -k_3 & 1 \\ 0 & 0 & c_2 & 0 & -c_1 \end{pmatrix}, \tag{58}$$

and the eigenvalues of the matrix (58) are:

$$\begin{array}{rcl} \lambda_{1,2,3,4} & = & -\mu, -k_2, -k_3, -c_1 \\ \lambda_5 & = & -k_1 + k_4\left(1 - \frac{\mu B}{\Lambda k_3}\right) \end{array} \tag{59}$$

where the eigenvalues $\lambda_{1,2,3,4}$ are negative. Therefore, the disease-free equilibrium point is locally asymptotically stable if and only if the following condition is fulfilled:

$$\frac{k_4}{k_1}\left(1 - \frac{\mu B}{k_3 \Lambda}\right) = \frac{\beta(1-p)}{\gamma_1 + \mu}\left(1 - \frac{\mu(c_3 + f)}{c_1(\rho + \mu)\Lambda}\right) < 1 \tag{60}$$

as it was demonstrated with the next generation matrices. □

Remark 3. *Consider the following characteristics:*

(i) *Taking into account the obtained $\mathcal{R}_c$, $\mathcal{R}_0$ is achieved with $B = 0$ (i.e., $\mathcal{R}_0 = \frac{\beta(1-p)}{\gamma_1+\mu}$). In such a case, P_{df}^{nv} is locally asymptotically stable if the transmission rate value is less than $\beta_c = \frac{\mu+\gamma_1}{1-p}$ (critical transmission rate without vaccination). Since the transmission rate is proportional to the contact rate c, see expression (2), the condition $\beta < \beta_c$ could be guaranteed by reducing the contact rate (e.g., imposing quarantine periods or reducing people's mobility).*

(ii) *When comparing $\mathcal{R}_0$ with $\mathcal{R}_c$, it is evident that vaccination ($B \neq 0$) permits greater transmission rates and therefore contact rates, too; if vaccination measurements are being implemented, one can calculate $\beta_{cc} = \frac{(\gamma_1+\mu)(\rho+\mu)\Lambda}{(1-p)[(\rho+\mu)\Lambda-\mu B]}$ (critical transmission rate with vaccination), which can be rewritten in terms of β_c; that is, $\beta_{cc} = \beta_c \frac{(\rho+\mu)\Lambda}{(\rho+\mu)\Lambda-\mu B}$. Therefore, if $B \neq 0$ and $B < \frac{\Lambda(\rho+\mu)}{\mu}$, it is straightforward that $\beta_{cc} > \beta_c$.*

(iii) *If the probability of being hospitalized is considered null (i.e., $p = 0$) and no vaccination is being applied, then an SIR model is obtained. In this particular case, $\mathcal{R}_0$ is reduced to $\mathcal{R}_0' = \frac{\beta}{\gamma_1+\mu}$, which corresponds to the basic reproduction number attained for an SIR model [7].*

(iv) The nominator of H_{ee}, see (36), can be rewritten in terms of $\mathcal{R}_c$;

$$n_H = \Lambda p(\rho+\mu)(\gamma_1+\mu)^2(1-\mathcal{R}_c). \tag{61}$$

Since it was proved that the denominator of H_{ee} is negative as far as $\gamma_1+\mu < \beta(1-p)$, then the existence of H_{ee} is ensured if $n_H < 0$, which corresponds with $\mathcal{R}_c > 1$. Therefore, when $\mathcal{R}_c < 1$, P_{df} as well as being locally asymptotically stable is the system's (3) unique attractor. When $\mathcal{R}_c > 1$, P_{df} turns unstable, and P_{ee} is reachable.

Proposition 4. *Assume that the disease-free equilibrium point is reachable. Then, it is marginally stable if and only if the control parameters are chosen such that:*

$$\mathcal{R}_c = \frac{\beta(1-p)}{\gamma_1+\mu}\left(1-\frac{\mu(c_3+f)}{c_1(\rho+\mu)\Lambda}\right) = 1. \tag{62}$$

3.2. Global Stability of the Disease-Free Equilibrium Point

With the aim of analyzing the global stability of the disease-free equilibrium point, first, the non-existence of a periodic solution will be proved, and secondly, the conditions for the global stability will be exposed.

Proposition 5. *Assume that $\beta < \beta_c = \frac{\mu+\gamma_1}{1-p}$, $f(t) = f$ for all $t \in [0,\infty)$, and $c_1 \geq \frac{\mu(c_3+f)}{\Lambda(\rho+\mu)}$. Then, the non-seriously infected and the hospitalized subpopulations vanish asymptotically. The above result still holds if $f(t)$ is picewise continuous with finite jump discontinuities on a finite real interval, $f(t) \to f^*$ as $t \to \infty$ and $c_1 > \frac{\mu(c_3+f^*)}{\Lambda(\rho+\mu)}$.*

Proof of Proposition 5. One obtains from $I(t)$ in (26) that if

$$\frac{\mu+\gamma_1}{\beta(1-p)} > \limsup_{t\to\infty}\frac{S(t)}{N(t)}, \tag{63}$$

then $I(t) \to 0$ as $t \to \infty$ for any finite $I(0) \geq 0$, then any periodic solution of $I(t)$ is neglected. Since, from Theorem 1, $S(t)/N(t) \leq 1$ for all $t \in [0,\infty)$ as all the subpopulations are non-negative and bounded for all $t > 0$ for any non-negative initial conditions.

The above condition is guaranteed if

$$\frac{\mu+\gamma_1}{\beta(1-p)} > 1, \tag{64}$$

that is, if $\beta < \beta_c$. Note from (55) that if $f(t) = f$ for all $t \in [0,\infty)$ then

$$\mathcal{R}_c = \frac{\beta(1-p)}{\mu+\gamma_1}\left(1-\frac{\mu(c_3+f)}{c_1\Lambda(\rho+\mu)}\right) \leq \frac{\beta(1-p)}{\mu+\gamma_1} \tag{65}$$

provided that $c_1 \geq \frac{\mu(c_3+f)}{\Lambda(\rho+\mu)}$ and if $\beta < \beta_c$ then $\mathcal{R}_c < 1$. Also, from $H(t)$ in (26),

$$H(t) = H(t_0)e^{-(\mu+\gamma_2+\alpha)(t-t_0)} + \int_{t_0}^{t} e^{-(\mu+\gamma_2+\alpha)(t-\tau)}\left(\frac{\beta I(\tau)S(\tau)p}{N(\tau)}\right)d\tau, \tag{66}$$

and the properties of the upper limits lead to the following inequality:

$$\limsup_{t\to\infty} H(t) \leq \limsup_{t\to\infty} H(t_0)e^{-(\mu+\gamma_2+\alpha)(t-t_0)} + \limsup_{t\to\infty}\int_{t_0}^{t} e^{-(\mu+\gamma_2+\alpha)(t-\tau)}\left(\frac{\beta I(\tau)S(\tau)p}{N(\tau)}\right)d\tau, \tag{67}$$

and considering a finite and non-negative initial condition $H(t_0)$, it follows that:

$$\limsup_{t\to\infty} H(t) \leq \limsup_{t\to\infty}\int_{t_0}^{t} e^{-(\mu+\gamma_2+\alpha)(t-\tau)}\left(\frac{\beta I(\tau)S(\tau)p}{N(\tau)}\right)d\tau. \tag{68}$$

Now, let us rewrite the expression for $H(t)$ for a time $t' = t + \Delta$ where Δ is finite and positive. Thus,

$$H(t+\Delta) = H(t)e^{-(\mu+\gamma_2+\alpha)\Delta} + \int_t^{t+\Delta} e^{-(\mu+\gamma_2+\alpha)(t+\Delta-\tau)}\left(\frac{\beta I(\tau)S(\tau)p}{N(\tau)}\right)d\tau, \tag{69}$$

and its upper limit

$$\limsup_{t\to\infty} H(t+\Delta) \leq \limsup_{t\to\infty} H(t)e^{-(\mu+\gamma_2+\alpha)\Delta} + \limsup_{t\to\infty} \int_t^{t+\Delta} e^{-(\mu+\gamma_2+\alpha)(t+\Delta-\tau)}\left(\frac{\beta I(\tau)S(\tau)p}{N(\tau)}\right)d\tau. \tag{70}$$

Since $\limsup_{t\to\infty} H(t) \leq \limsup_{t\to\infty} H(t+\Delta)$, it yields

$$\limsup_{t\to\infty} H(t) \leq \frac{1}{1-e^{-(\mu+\gamma_2+\alpha)\Delta}} \limsup_{t\to\infty} \int_t^{t+\Delta} e^{-(\mu+\gamma_2+\alpha)(t+\Delta-\tau)}\left(\frac{\beta I(\tau)S(\tau)p}{N(\tau)}\right)d\tau. \tag{71}$$

In Theorem 1, it was proved that $S(t)$ and $N(t)$ are bonded, then if $I(t) \to 0$ as $t \to \infty$, one has that:

$$\limsup_{t\to\infty} H(t) = 0. \tag{72}$$

Since in Theorems 1 and 2 it was proved that $H(t)$ is non-negative, the following limit exists:

$$\lim_{t\to\infty} H(t) = \limsup_{t\to\infty} H(t) = 0. \tag{73}$$

The first part of the result for constant $f(t)$ has been proved. If now $f(t) \to f^*$ ($f(t)$ tends asymptotically to f^*) and it is picewise continuous with bounded jump discontinuities, then for any given real $\epsilon > 0$, there is some finite $t_1 = t_1(\epsilon)$ such that $f(t) \leq f^* + \epsilon$, for all $t \geq t_1$. Then, the above results hold if $c_1 \geq \frac{\mu(c_3+f^*+\epsilon)}{\Lambda(\rho+\mu)}$ since $\epsilon > 0$ is arbitrary, and it suffices that $c_1 > \frac{\mu(c_3+f^*)}{\Lambda(\rho+\mu)}$. □

Remark 4. *If the vaccination (5) is performed with c_1, the gain of the vaccination dynamics is sufficiently large and $f(t)$ is constant, then the basic reproduction number is less than unity, and the disease-free equilibrium point is locally asymptotically stable. Moreover, if it is assumed that $\beta < \beta_c$, β_c is the critical disease transmission threshold, the disease-free equilibrium point is unique (independently of the vaccination tuning parameters, the endemic equilibrium point is not reachable; see Proposition 2), then the above proposition ensures that the disease-free equilibrium point is also globally asymptotically stable.*

3.3. Local Stability of the Endemic Equilibrium Point

Theorem 4. *Assume that there is no vaccination, and that the P_{ee}^{nv} is reachable. Then, the endemic equilibrium point is locally asymptotically stable and the P_{df}^{nv} is unstable.*

Proof Outline of Theorem 4. To proof the local stability of P_{ee}^{nv} (i.e., $c_1 = c_2 = c_3 = f = 0$), system (3) has been linearized about P_{ee}^{nv} given in (49), and the Jacobian matrix has been obtained. Due to the system's complexity, instead of calculating directly its eigenvalues, the Routh–Hurwitz criterion has been applied, which determines the conditions for the existence of eigenvalues with positive real parts. From the Routh–Hurwitz criterion, and assuming that $\gamma_1 + \mu < \beta(1-p)$, it is concluded that the equilibrium point is locally asymptotically stable. More details are given in Appendix A. □

Theorem 5. *Assume that a vaccination exists and that P_{ee} point is reachable. Then, P_{df} is unstable, and given any c_1, c_3, and f, the endemic equilibrium point is locally asymptotically stable if c_2 fulfills the following conditions:*

$$c_2 < \frac{c_1\{k_1k_2\mu + \rho[p\gamma_1(\alpha+\mu) + (1-p)\gamma_2\mu + \mu(\alpha+\mu)] - k_1k_3p\alpha\frac{\mathcal{R}_c}{\mathcal{R}_0}\}}{k_1p\mu}, \tag{74}$$

$$c_2 \sup_{\omega\in\mathbb{R}_+}\left(\frac{|\Delta f(i\omega)|}{|f(i\omega)|}\right) < 1, \tag{75}$$

where $\mathbb{R}_+ = \{x \in \mathbb{R} : x \geq 0\}$. In addition,

$$\begin{aligned} f(\lambda) &= d_{i1}(\lambda^4 + a_3\lambda^3 + a_2\lambda^2 + a_1\lambda + a_0)(\lambda + c_1), \\ \Delta f(\lambda) &= (\lambda+\mu)\Big[\tfrac{\mathcal{R}_0k_1p\mu}{c_1}(\lambda+k_3)(\lambda+k_2)(\lambda+c_1)\lambda + p\beta n_i(1-s_{ee})(\lambda+k_1)\Big], \end{aligned} \tag{76}$$

and

$$\begin{aligned} n_i &= (\gamma_2+\alpha+\mu)(\rho+\mu)(1-p)\mu(\mathcal{R}_c-1), \\ d_{i1} &= \mathcal{R}_0\{(\gamma_1+\mu)(\gamma_2+\alpha+\mu)\mu + \rho[p\gamma_1(\alpha+\mu) + (1-p)\gamma_2\mu + \mu(\alpha+\mu)] - (\gamma_1+\mu)(\rho+\mu)p\alpha\tfrac{\mathcal{R}_c}{\mathcal{R}_0}\}, \\ a_3 &= \beta\tfrac{n_i}{d_{i1}} + \gamma_2 + \alpha + \rho + 3\mu, \\ a_2 &= \beta\tfrac{n_i}{d_{i1}}[\gamma_1 + \alpha + \gamma_2 + \rho + 3\mu - \alpha p s_{ee}] + \mu(\rho+\mu) + (\gamma_2+\alpha+\mu)(\rho+2\mu), \\ a_1 &= \beta\tfrac{n_i}{d_{i1}}[(\gamma_1+\rho+2\mu)(1-ps_{ee})\alpha + [p\gamma_1 + (1-p)\gamma_2 + 2\mu]\rho + (\gamma_1+2\mu)(\gamma_2+\mu) + (\gamma_1+\mu)\mu] + \mu(\gamma_2+\alpha+\mu)(\rho+\mu), \\ a_0 &= \beta\tfrac{n_i}{d_{i1}}\{(\gamma_1+\rho+\mu)(1-ps_{ee})\alpha\mu + p(1-s_{ee})\gamma_1\alpha\rho + (1-p)\gamma_2\rho\mu + [(\gamma_1+\mu)\gamma_2 + (p\rho+\mu)\gamma_1 + (\rho+\mu)\mu]\mu\}. \end{aligned} \tag{77}$$

Proof Outline of Theorem 5. To prove the local stability of P_{ee}, as in the proof of Theorem 4, from the linearized system (3) about P_{ee} given in (36), the characteristic equation has been obtained, and it has been rewritten as the sum of two polynomials whose roots location is known. Finally, from Rouche's theorem [47], the conditions which ensure that all roots are located in the open left-half plane (they have a negative real part), so the system is locally asymptotically stable, have been inferred. More details are given in Appendix B. □

Remark 5. *Taking into account Theorem 5 and the conditions (74) and (75), the following hold:*

(i) Conditions (74) and (75) are sufficient conditions; that is, if they are fulfilled, the stability of the endemic equilibrium point is ensured. Contrary, if the conditions are not fulfilled, the stability of the equilibrium point is not guaranteed.

(ii) Taking into account condition (74), and considering that it is proportional to c_1, let $c_1 \to 0$; then, the endemic equilibrium point is stable if $c_2 \to 0$ regardless of the condition (75), which is in accordance with Theorem 4. In addition, bigger values of c_1 allow bigger values of c_2.

(iii) The conditions (74) and (75) can be unified on a single condition; that is,

$$c_2 < \bar{c}_2 = \min\left\{\frac{c_1\{k_1k_2\mu + \rho[p\gamma_1(\alpha+\mu) + (1-p)\gamma_2\mu + \mu(\alpha+\mu)] - k_1k_3p\alpha\frac{\mathcal{R}_c}{\mathcal{R}_0}\}}{k_1p\mu}, \frac{1}{\sup_{\omega\in\mathbb{R}}\left(\frac{|\Delta f(i\omega)|}{|f(i\omega)|}\right)}\right\}, \tag{78}$$

which, from a numerical point of view, can easily be computed. Once all the parameters are defined, the values of c_1, c_3, and f can be chosen so $\mathcal{R}_c > 1$, and then the condition (74) can be computed. Finally, to obtain a numerical value of the second condition, from the bode magnitude plot of $|G(i\omega)| = \frac{|\Delta f(i\omega)|}{|f(i\omega)|}$, it is possible to obtain its peak value G_{max} and calculate the condition (75). Finally, the minimum between both results will be chosen.

Proposition 6. *Assume that the endemic equilibrium point is reachable and*

$$\beta \to \beta_{cc} = \left(\frac{\mu+\gamma_1}{1-p}\right)\left(\frac{(\rho+\mu)\Lambda}{(\rho+\mu)\Lambda - \mu B}\right), \tag{79}$$

so $\mathcal{R}_c \to 1$. *Then, the endemic equilibrium point is marginally stable.*

Proof of Proposition 6. $\mathcal{R}_c \to 1$ implies $i_{ee} \to 0$, so the eigenvalues problem exposed in Appendix B is reduced to

$$\lambda(\lambda + c_1)\left[\lambda^3 + (\gamma_2 + \alpha + \rho + 3\mu)\lambda^2 + (\mu(\rho + \mu) + (\gamma_2 + \alpha + \mu)(\rho + 2\mu))\lambda + \mu(\gamma_2 + \alpha + \mu)(\rho + \mu)\right] = 0 \quad (80)$$

From Equation (80), two roots are directly derived; $\lambda_{1,2} = 0, -c_1$. Regarding the remaining roots, with the Routh–Hurwitz stability criterion, it can be easily proved that all their real parts are negative. □

Remark 6. *In Remark 1, point (iv), it is noted that* P_{ee} *tends to* P_{df} *when* $\mathcal{R}_c \to 1$. *In addition, in Proposition 4, it is stated that* P_{df} *is marginally stable when* $\mathcal{R}_c = 1$. *Then, it is clear that Proposition 6 is consistent with the previous results.*

3.4. Stability of the Endemic Equilibrium Point

Taking into account the definition of stability given in [48], one obtains the subsequent result.

Proposition 7. *Assume that the endemic equilibrium point is reachable, then it is stable at time* t_0.

Proof of Proposition 7. It is possible to determine the bound of the initial conditions $\boldsymbol{\delta}(t_0)$ as $\mathbf{D}$, see (19), such that any solution of (3) starting at t_0 always lies inside $\boldsymbol{\epsilon} > \mathbf{0}$ (one can simply choose $\boldsymbol{\delta} = \boldsymbol{\epsilon}$) at all times $t \geq t_0$; that is, considering $\boldsymbol{x}(t)$ and $\boldsymbol{x}^*$ as the solution and the equilibrium point, respectively, of system (3), it follows that:

$$\|\boldsymbol{x}(t_0) - \boldsymbol{x}^*\| < \boldsymbol{\delta}(t_0) \implies \|\boldsymbol{x}(t) - \boldsymbol{x}^*\| < \boldsymbol{\epsilon},\ \forall\, t \geq t_0. \quad (81)$$

With $\boldsymbol{\delta}(t_0) = \boldsymbol{\epsilon} = \mathbf{D}$, (81) holds. □

4. Simulations

Some simulations have been carried out to validate the results obtained in the previous sections. The parameter values have been gathered from different sources; regarding the natural birth and death rate, the Spanish public source Instituto Nacional de Estadística (National Statistics Institute) [40] has been used. In a survey where 28,503 people participated [41], their contact rate with respect to their incomes, locations, age, etc. was analyzed, and they showed an overall value of 14.5 contacts per day. The transmission probability has been proved to vary in different settings [42]; that is, in cases in which the contact is more prolonged, the transmission probability value can reach the 21.1%, and in working places, it decreases to 1.9%. It has been observed that the hospitalization risk among the COVID-19 patients in England changes notoriously between groups, being the greatest (39.5%) in the elderly population (80 years or older), and in the case of a medium-age population (40–49 years), the probability decreases to 19.1% [43]. In addition, all age groups achieve a peak value in winter months, which is a trend that may be caused by a weakener health system during this period. Regarding hospitalized people's recovery and death rates, confirmed COVID-19 cases from Belgium are processed in [44], and it is concluded that people around 20–60 years old stay 8.2 days in the hospital until they recover. In addition, on average, they stay 12.2 days until they die. With respect to the duration of immunity, the immunity wanes after 3–24 weeks after vaccination, and is not until the 24th week that there is an important decline in immunity [45]. Based on available data, Table 1 shows a summary of the parameter values used for simulation proposes within their respective references. Note that depending on the analysis, the contact rate (c) will be modified.

Table 1. Values of the model parameters.

Parameter	Definition	Value	Cite
c	Contact rate	$14.5\,\text{day}^{-1}$	[41]
p_i	Transmission probability of not serious infected people	0.211	[42]
p	Hospitalisation probability	0.16	[43]
μ	Natural death rate	$2.282 * 10^{-5}\,\text{day}^{-1}$	[40]
γ_1	Non-seriously infected recovery rate	$0.13\,\text{day}^{-1}$	[49]
γ_2	Hospitalized people recovery rate	$0.12\,\text{day}^{-1}$	[44]
α	Disease-induced death rate	$0.082\,\text{day}^{-1}$	[41]
ρ	Immunity lose rate	$0.006\,\text{day}^{-1}$	[45]

Considering the parameters given in Table 1, the condition $\gamma_1 + \mu < \beta(1-p)$ is fulfilled, and by substituting their values into the denominator of H_{ee}, see (36), one obtains:

$$d_H = k5 + k6 - A\mu k_4 p k_1 = -1.6177 * 10^{-5} - 6.597 * 10^{-8}(14.0789 + A), \quad (82)$$

which is negative as far as $A \geq 0$, as it was seen in the *proof* of Proposition 3.

One can rewrite the nominator of H_{ee} in terms of $\mathcal{R}_c$:

$$(\Lambda k_3(k_1 - k_4) + \mu k_4 B)pk_1 = \Lambda k_3 p k_1^2(1 - \mathcal{R}_c) = \Lambda p(\rho + \mu)(\mu + \gamma_1)^2(1 - \mathcal{R}_c), \quad (83)$$

and in agreement with the statement exposed in Remark 3, from (82) and (83), it is concluded that the endemic equilibrium point is reachable (unrechable) when $\mathcal{R}_c > 1$ ($\mathcal{R}_c < 1$).

The simulations have been carried out with the version R2022a of Matlab, and the differential equations shown in (3) have been solved with the solver *ode45()*, where the selected time step has been 1 day; that is, all the results regarding the epidemic evolution (any subpopulation or vaccine evolution) are given in discrete form, which are equally spaced data points in time (i.e., 1 day). For the graphical representation, the function *plot()*, which generates a line plot from the data points, has been used. Note that in the interest of clarity in data visualization, the function *plot()* has been applied instead of *stem()*, which is used to plot discrete sequence data.

Since in Section 3.2, it was proved that the disease-free equilibrium point is globally asymptotically stable under certain conditions, in the following simulations, this characteristic will be verified, and subsequently other simulations will be executed for the local asymptotic stability analysis. With regard to the endemic equilibrium point, with and without vaccination, the condition for its stability will be evaluated for different c_1 values, and it will be verified that the requirements given in Theorem 5 are accomplished. In Section 4.3, the state feedback vaccination method is compared with other common vaccination methods based on the hospitalized subpopulation and vaccination evolution. Finally, a vaccination specification is defined, and the tuning parameters are set up to match the desired specification.

4.1. Stability of the Disease-Free Equilibrium Point

4.1.1. Global Stability

Firstly, the condition (32) shown in Proposition 1, which ensures the existence of P_{df}, has been considered (i.e., $B \leq B_{df} = 1.642 * 10^5$). Consequently, by establishing $B = 1.410 * 10^5$, the condition is fulfilled and P_{df} is reachable. Then, the conditions for the global stability have been considered, see Proposition 5; taking into account that $\beta < \beta_c = 0.15$ must be fulfilled (first condition), with $\beta = 0.14$, the requirement is satisfied, and it leads to the contact rate $c = 0.663$ (for the simulation carried out in this subsection,

instead of using the value of the contact rate shown in Table 1, the value 0.0663 has been used). With $c_3 = f = B/2 = 70500$, it follows that $c_1 > 0.082$ (second condition). Consequently, if one chooses $c_1 = 1$, the second condition is fulfilled and P_{df} is globally stable. With $A = c_2/c_1 = 0 \implies c_2 = 0$, all parameters needed for simulation purposes have been already defined. Regarding the initial conditions, it has been assumed that there is a low quantity of non-seriously infected and hospitalized people and that nobody has been vaccinated yet; that is, $S(0) = 46 * 10^6$, $I(0) = 1000$, $H(0) = 50$, $R(0) = 0$, and $v(0) = 0$. Then, the epidemic evolution has been simulated; see Figure 2.

As it was expected from the theoretical results, it can be observed that all the subpopulations tend asymptotically to the disease-free equilibrium value. After 37 days the number of hospitalized people is reduced to less than one, and after 30 days, the same happens with the infected individuals. During this period, 404 people die as a consequence of the disease. This type of epidemic evolution is always desired, since the the number of infected and hospitalized individuals decay rapidly to zero regardless the outbreak magnitude. However, the social effort needed for this propose is high; considering that $p_i = 0.211$, the contact rate must be reduced to less than 0.7 contacts per day so that $\beta < \beta_c$, which implies self-isolation.

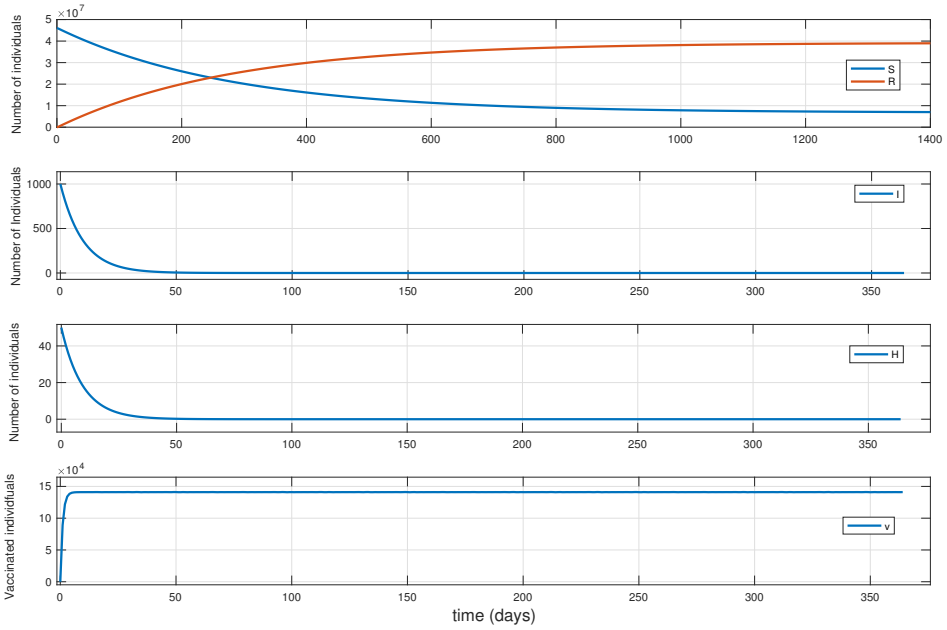

Figure 2. Evolution of all subpopulations and vaccinations when the conditions for global asymptotic stability of the disease-free equilibrium point (P_{df}) are fulfilled ($\beta = 0.14$, $c_1 = 1$, $c_2 = 0$ and $c_3 = f = 70500$).

4.1.2. Local Stability

As it was previously seen, P_{df} is reachable with $B < B_{df} = 1.642 * 10^5$. Now, the most common way to achieve a $\mathcal{R}_c$ lower than one, so P_{df} is locally asymptotically stable, is to modify the contact rate or/and the vaccination tuning parameters. Considering the contact rate given in Table 1, and supposing that its value is fixed, in the following two simulations, the asymptotic stability will be analyzed with respect to the different vaccination tuning parameters. For both simulations, it has been assumed that initially, R is big compared to S; $S(0) = 7.42 * 10^6$, $I(0) = 1000$, $H(0) = 50$, $R(0) = 40 * 10^6$, and $v(0) = 1000$.

- From the condition $R_c > 1$, so P_{df} is unstable, it follows that $B < 1.5606 * 10^5$: for $c_2 = 0.01$, $c_3 = f = 5500$, and $c_1 = 0.1$, one obtains that $B = 1.1 * 10^5$ and $\mathcal{R}_c = 6.64$. The epidemic evolution shown in Figure 3 is obtained where the subpopulations do not reach P_{df}, but P_{ee}: $S_{ee} = 1.66 * 10^6$, $I_{ee} = 2.84 * 10^4$, $H_{ee} = 3.39 * 10^3$, $R_{ee} = 3.18 * 10^7$ and $v_{ee} = 1.10 * 10^3$. This is a predictable result since, for the parameters itemized in Table 1, P_{ee} is reachable when $\mathcal{R}_c > 1$.

- From the condition $R_c \leq 1$, so P_{df} is locally asymptotically stable, it follows that $B \geq 1.5606 * 10^5$. With $c_2 = 0.01$, $c_3 = f = 7850$, and $c_1 = 0.1$, $B = 1.57 * 10^5$ and $\mathcal{R}_c = 0.8846$ are attained. The resulting epidemic evolution has been depicted in Figure 4, where one can see that the model tends to P_{df}; after 164 days approximately, the non-seriously infected and the hospitalized subpopulations are less than one, and some time after, S and R reach the points $S_{df} = 2.282 * 10^6$ and $R_{df} = 4.3682 * 10^7$, respectively, as expected.

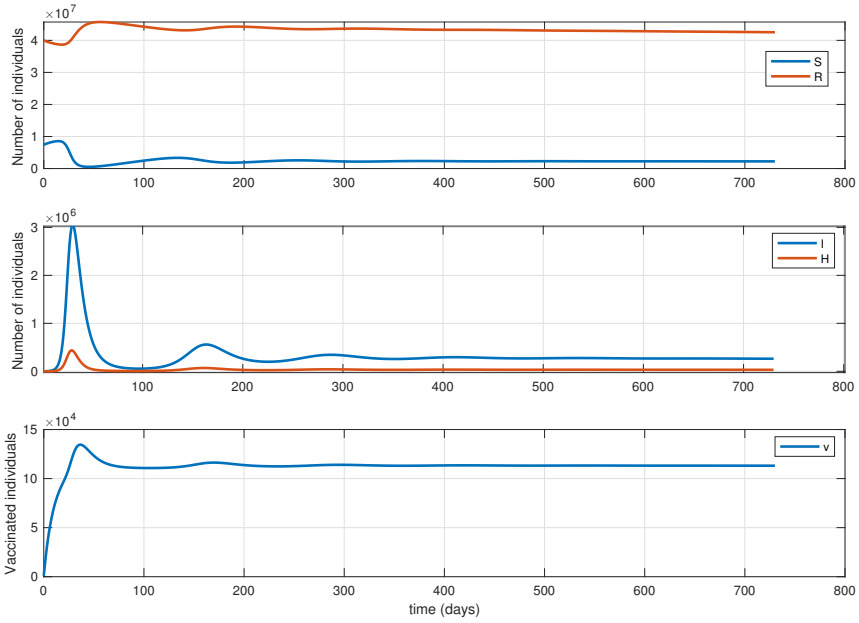

Figure 3. Evolution of the whole subpopulations and vaccinated individuals when the conditions for local asymptotic stability of P_{df} are not fulfilled. The values of the vaccination tuning parameters are $c_1 = 0.1$, $c_2 = 0.01$ and $c_3 = f = 5500$.

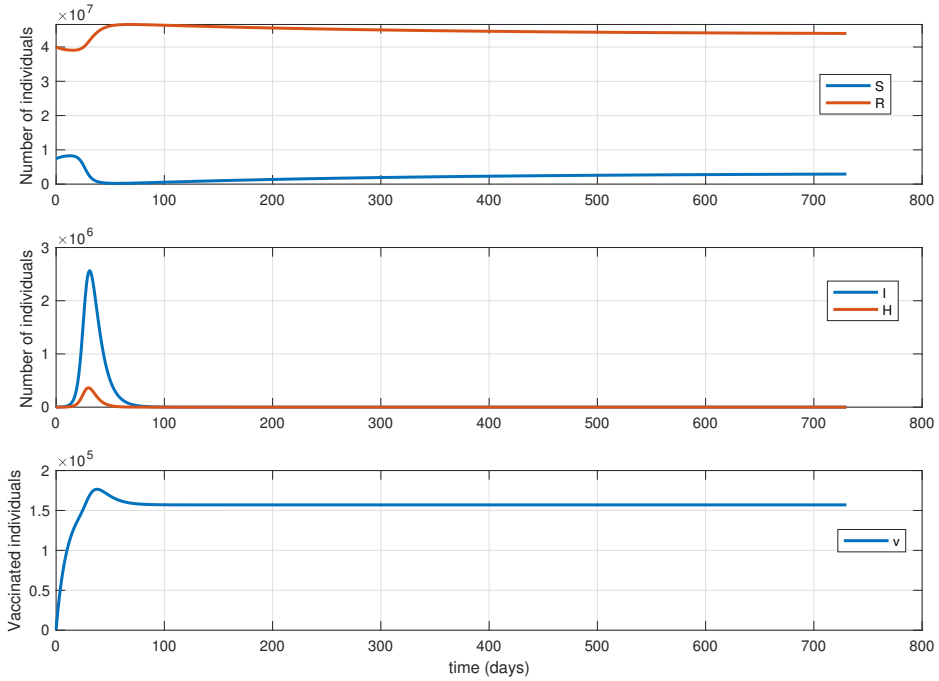

Figure 4. Evolution of the whole subpopulations and vaccinations when the conditions for local asymptotic stability of P_{df} are fulfilled. The values of the vaccination tuning parameters are $c_1 = 0.1$, $c_2 = 0.01$ and $c_3 = f = 7850$.

In Table 2, some data of interest regarding previous simulations are summarized.

Table 2. Epidemic evolution's significant features.

	$\mathcal{R}_c = 6.64$		$\mathcal{R}_c = 0.88$	
	Time (Days)	**Individuals**	**Time (Days)**	**Individuals**
v_{peak}	38	134.550×10^3	39	176.580×10^3
H_{peak}	30	436.770×10^3	31	363.290×10^3
deaths peak	30	35.801×10^3	31	29.778×10^3
total vaccines	0–730	82.096×10^6	0–730	113.750×10^6
total deaths	0–730	2.3467×10^6	0–730	509.220×10^3

During the first days, when the infected subpopulation starts to increase again, even if the differences between both cases are minor, it is observed that a higher vaccination helps to avoid future deaths. At the end of 2 years, the differences between both cases are more notorious; when $\mathcal{R}_c = 0.88$, the total vaccination is 1.3% higher than the total vaccination in $\mathcal{R}_c = 6.64$, whereas the total deaths decreases four times.

The simulations of these particular cases are significant because the initial conditions are comparable to the current COVID-19 epidemic situation, and they highlight the importance of maintaining $\mathcal{R}_c < 1$, since it avoids a significant increment in the total number of deaths.

4.2. Stability of the Endemic Equilibrium Point

4.2.1. Local Stability without vaccination

Theorem 4 states that if P_{ee}^{nv} is reachable (i.e., $\gamma_1 + \mu < \beta(1-p)$), then it is locally asymptotically stable. With the objective of reinforcing this theorem, the terms from the Routh tablet (d_1^{nv} and g_1^{nv}) given in (A7), Appendix A, can be evaluated numerically for different β values and verify its stability; if the terms are positive, then P_{ee}^{nv} is locally asymptotically stable. Whereas, if any term is negative, then P_{ee}^{nv} is unstable. Considering the parameter values given in Table 1, the terms in (A7) have been evaluated for different β values, and the result is depicted in Figure 5.

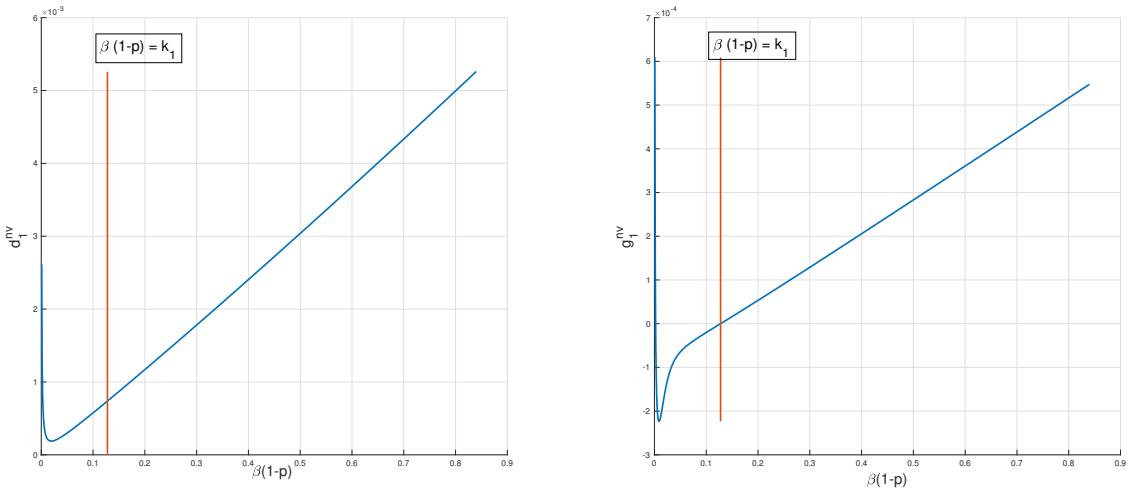

Figure 5. The blue lines stand for the graphical representation of the terms in (A7), which determine the local asymptotic stability of the endemic equilibrium point without vaccination (P_{ee}^{nv}) with respect to $\beta(1-p)$. Note that only the values at the right side of the red lines, which represent $\beta(1-p) = k_1$ for any d_1^{nv} (left graph) and g_1^{nv} (right graph), must be considered.

In Figure 5, a red line is also shown to emphasize that only the values of d_1^{nv} and g_1^{nv} that correspond to $\beta(1-p) > \gamma_1 + \mu$ must be taken into account. As it was expected from the theoretical results, d_1^{nv} and g_1^{nv} are positive if $\beta(1-p) > \gamma_1 + \mu$.

4.2.2. Local Stability with Vaccination

Theorem 5 states that it is sufficient if the conditions (74) and (75) are fulfilled to ensure the local asymptotic stability of P_{ee}. In this section, the procedure to compute the condition for c_2, which is exposed in Remark 5, will be followed.

Let us consider the parameters given in Table 1 and the following vaccination tuning parameters values $c_1 = 0.1$ and $c_3 = f = 736.05$, so $\mathcal{R}_c = 2.08 > 1$ (P_{df} is not locally asymptotically stable). Then, the condition (74) has been computed:

$$c_2 < 25.7206. \tag{84}$$

To calculate the numerical value for the second condition, see expression (75), the bode magnitude plot of the function $|G(i\omega)| = \frac{|\Delta f(i\omega)|}{|f(\omega)|}$ has been computed, which is shown in Figure 6. From Figure 6, the peak has been obtained, which corresponds to 22.7093 dB. Thus,

$$c_2 < 0.0732. \tag{85}$$

Finally, the minimum value between the values given in (84) and (85) has been chosen; $c_2 < \bar{c}_2 = 0.0732$.

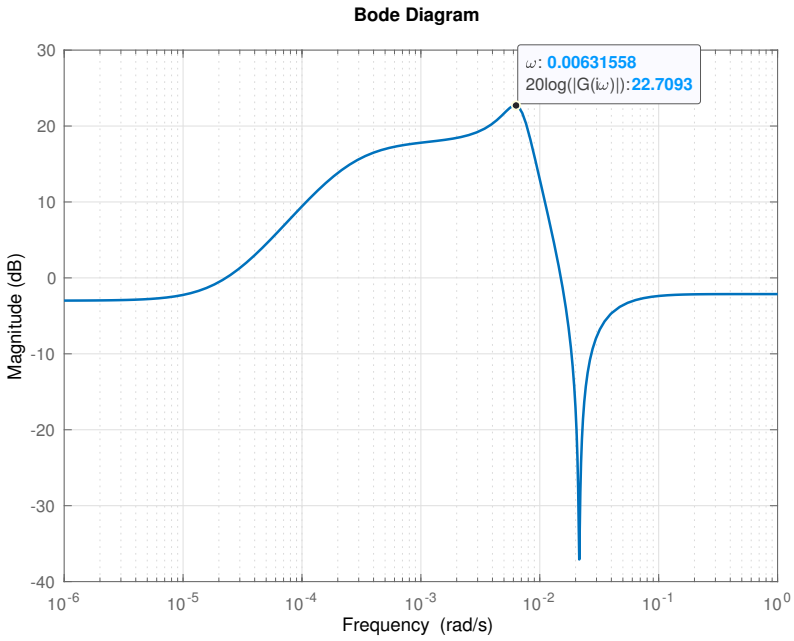

Figure 6. Bode magnitude diagram of $|G(i\omega)|$, see Equation (75), given the parameters shown in Table 1, and the vaccination tuning values $c_1 = 0.1$ and $c_3 = f = 736.05$.

The roots of the characteristic equation obtained from the linearized system (3) about P_{ee}, see Equation (A12), have been computed for different c_2 cases; $c_2 < \bar{c}_2$, $c_2 = \bar{c}_2$ and $c_2 > \bar{c}_2$. See Table 3 for more details.

Table 3. Roots of the characteristic equation, see expression (A12) in Appendix B, for different c_2 cases when $c_1 = 0.1$ and $c_3 = f = 736.05$.

Roots	$c_2 = 0.007$	$c_2 = 0.073$	$c_2 = 0.73$
r_1	-2.2552×10^{-4}	-1.5916×10^{-4}	-5.551×10^{-5}
r_2	$-0.0171 - 0.0641i$	$-0.0089 - 0.069i$	$0.0083 - 0.0758i$
r_3	$-0.0171 + 0.0641i$	$-0.0089 + 0.0069i$	$0.0083 + 0.0758i$
r_4	-0.1009	-0.1058	-0.113
r_5	-0.2046	-0.2093	-0.220

Taking into account the results in Table 3, variations in c_2 barely affect r_4 and r_5. In the case of r_1, r_2, and r_3, when c_2 increases, their real parts decrease (the time for the response to reach the final value will be bigger), whereas the imaginary parts of r_2 and r_3 tend to increase (the response of the associated eigenvectors will be characterized by bigger oscillations). Regarding the stability, two of three are stable since all r_i, where $i = 1, 2, 3, 4.5$, have negative real parts. As it was mentioned in Remark 5, even if the condition $c < \bar{c}_2$ is not fulfilled, the system might still be stable since not fulfilling the conditions (74) and (75) does not imply that the equilibrium point will be unstable. However, when $c_2 = 0.073$, r_2 and r_3 have a positive real part and they are complex-conjugate poles. This instability is caused by the violation of the condition (i) given in Theorem 2 (i.e., $v(t) > \overline{v(t)}$).

4.3. Study of State Feedback Vaccination

To analyze the benefits of the state feedback vaccination method, its performance will be compared with that of other common vaccination control methods, such as the constant and the proportional methods. These controllers will be defined as follows.

$$\begin{aligned} v^{(1)} &= c_2^{(1)}, \\ v^{(2)} &= c_2^{(2)} H, \quad \text{and} \\ \dot{v}^{(3)} &= -c_1 v + c_2^{(3)} H. \end{aligned} \tag{86}$$

Note that $\dot{v}^{(3)}$ is the simplified version of the equation given in (5). In addition, $v^{(2)}$ and $v^{(3)}$ are functions of the state H, since it has been assumed that data exist regarding the hospitalized people, which makes its implementation possible. Each vaccination function will be set up to drive the hospitalized subpopulation to the desired value H^*, and each performance will be evaluated based on the following features: v_{peak}, H_{peak}, the total number of people who receive a vaccine dose up to 365 days, and the total number of deaths up to 365 days.

Let $P_{ee}^{(i)} = (S_{ee}^{(i)}, H_{ee}^{(i)}, I_{ee}^{(i)}, R_{ee}^{(i)})$ be the endemic equilibrium point belonging to $v^{(i)}$, where $i = 1, 2, 3$. Taking the parameter values in Table 1, $H_{ee}^{(i)}$ has been calculated, and the condition $H_{ee}^{(1)} = H_{ee}^{(2)} = H_{ee}^{(3)} = H^* = 1.067 * 10^4$ has led to $c_2^{(1)} = 7.68 * 10^3$, $c_2^{(2)} = 0.72$, and $c_2^{(3)} = c_1 c_2^{(2)}$ for $\forall c_1 > 0$. Two values of c_1 have been considered, $c_1 = 1$ and $c_1 = 0.1$, thereby giving $c_2^{(3)} = 0.72$ and $c_2^{(3)} = 0.072$, respectively. Then, with the initial conditions $S(0) = 10 * 10^6$, $I(0) = 1000$, $H(0) = 50$, $R(0) = 40 * 10^6$, and $v(0) = 0$, a simulation of the epidemic evolution has been carried out, and in Figure 7, the evolution of the hospitalized subpopulation per day and the number of vaccinated people per day has been displayed. Note that the settling time is bigger than 365 days, since none of the four cases reach the desired state H^* at the end of 1 year.

As it can be observed in Figure 7, with our state feedback controller, the vaccination performance can be modified; it is possible to switch from an underdamped-like behavior to an overdamped. Meanwhile, with $v^{(1)}$ and $v^{(2)}$, vaccination is totally conditioned by a constant value and H, respectively.

Taking into account the performance measurements given in Table 4, if the objective is to reduce as much as possible the number of deaths, then $v^{(2)}$ gives the best response while

$v^{(1)}$ gives the worst. However, these types of responses are usually difficult to implement (e.g., there could be staff limitations or cost limits), and in such cases, big vaccination peaks (e.g., the peaks observed with $v^{(2)}$, and $v^{(3)}$ when $c_1 = 1$) are not desired. By decreasing the value of c_1, $v^{(3)}$ can be adjusted to the desired response.

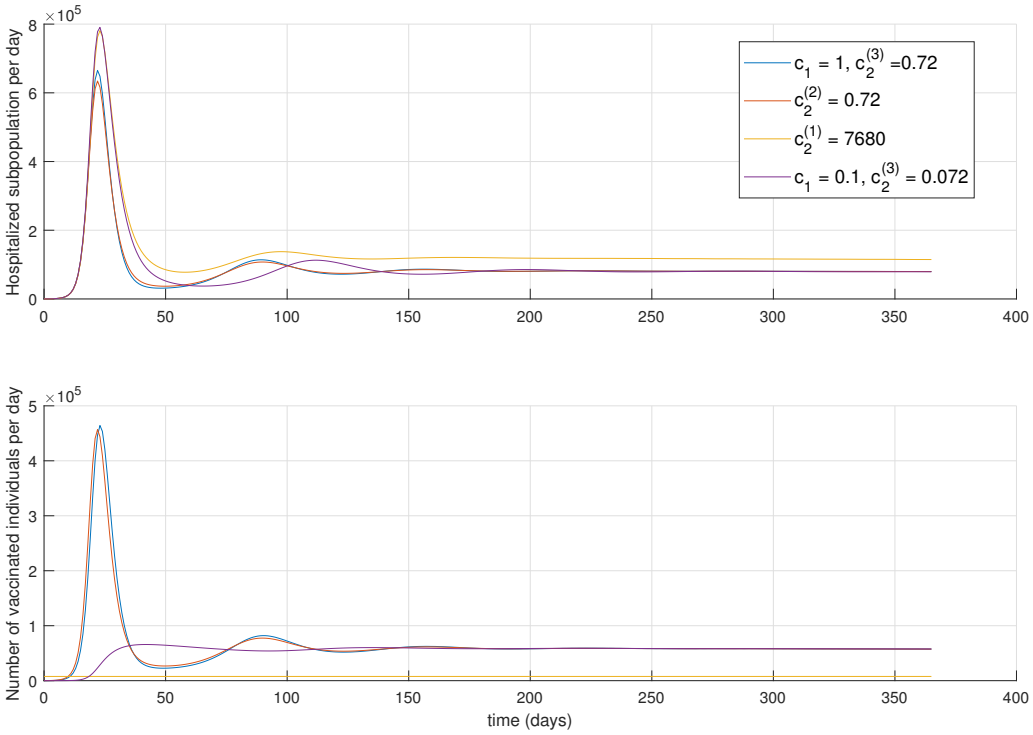

Figure 7. Evolution of infected hospitalized (H) subpopulation and vaccinated individuals (v), with respect to time, with the initial conditions $S(0) = 10 * 10^6$, $I(0) = 1000$, $H(0) = 50$, $R(0) = 40 * 10^6$, and different vaccination methods.

Table 4. Performance of different vaccination control methods.

	$v^{(1)}$	$v^{(2)}$	$v^{(3)}$	
	$c_2^{(1)} = 1.7 \times 10^4$	$c_2^{(2)} = 0.72$	$c_1 = 1,\ c_2^{(2)} = 0.72$	$c_1 = 0.1,\ c_2^{(2)} = 0.072$
v_{peak}	-	4.567×10^5	4.642×10^5	65,781
H_{peak}	7.811×10^5	6.344×10^5	6.65×10^5	7.905×10^5
total vaccines	2.810×10^6	2.387×10^7	2.383×10^7	2.006×10^7
total deaths	3.972×10^6	2.717×10^6	2.719×10^6	2.94×10^6

4.4. Study of Vaccination Strategy Design and Implications

For the proposal of a vaccination strategy, it will be assumed that the initial conditions are known and that v_d vaccines are delivered every T days:

$$v_d(t) = v_d\delta(t - (n-1)T) \ : \ n \in \mathbb{N}^+ \tag{87}$$

Then, the vaccines stock $v_s(t)$ can be defined as:

$$v_s(t) = \sum_{n=1}^{\infty} v_d\theta(t - (n-1)T) - \int_0^t v(\tau)d\tau, \tag{88}$$

where $n \in \mathbb{N}^+$, and $\theta(t)$ is the Heaviside function. Therefore, $v_s(t)$ is a picewise continuous with jump discontinuities.

During the period $(n-1)T \leq t < nT$, the vaccination strategy will be characterized by two main points:

- A continuous vaccination of about $v_s((n-1)T)/3T$: considering the expression for $v(t)$ in (24), the term $c_3(1-e^{-c_1 t})/c_1$ is a good candidate for this propose, since

$$\lim_{t\to\infty} \frac{c_3}{c_1}(1-e^{-c_1 t}) = \frac{c_3}{c_1}. \tag{89}$$

Therefore, $c_3/c_1 = v_s((n-1)T)/3T$. It is possible to define c_1 by imposing a condition related to the vaccination response; that is, if it is desired to reach $7/10$ of the vaccination final value (i.e., c_3/c_1) when $t = T/3$, then

$$c_1 = \frac{3}{T}\ln\left(\frac{10}{3}\right), \tag{90}$$

and consequently,

$$c_3 = \frac{v_s((n-1)T)}{T^2}\ln\left(\frac{10}{3}\right). \tag{91}$$

Note that c_3 depends on $v_s((n-1)T)$, whose value changes every period. Therefore, for every time period, c_3 must be updated before simulating the solution of system (3).

- As fast as there is a new vaccine delivery, an increment in vaccination is desired, and this rise must disappear with respect to time. This condition can be accomplished if one chooses $f(t)$ such that $f(t) = v_d\delta(t-(n-1)T)/2$. Thus, the term containing $f(t)$ in Equation (22) turns into

$$\int_{(n-1)T}^{t} e^{-c_1(t-\tau)} f(\tau)d\tau = \frac{v_d}{2}\int_{(n-1)T}^{t} e^{-c_1(t-\tau)}\delta(\tau-(n-1)T)d\tau = \frac{v_d}{2}e^{-c_1(t-(n-1)T)}. \tag{92}$$

Regarding c_2, different values will be used to see its implications.

Supposing that $T = 30$ days and $v_d = 6*10^6$, it leads to $c_1 = 0.1204$. With the initial conditions $S(0) = 7.42*10^6$, $I(0) = 1000$, $H(0) = 50$, $R(0) = 40*10^6$, and $v(0) = 0$, a simulation has been carried out for $n = 1,2,3,4,5$, and c_3 has been updated for each period; see Table 5 for more information. After repeating this procedure for different c_2 values, the results have been depicted (blue lines) in Figure 8. To show the advantage of vaccination strategy, Figure 8 also shows how infected and hospitalized individuals as well as the cumulative deaths evolve with respect to time when no vaccines are implemented (red lines). For each c_1, c_2, and c_3 combination, it has been checked that the number of vaccinated individuals never exceeds the vaccines stock nor the number of susceptible individuals, so Theorem 2 is not contradicted.

Table 5. Computed values of c_3 and $\mathcal{R}_c$ for the given time periods.

n	Time Period (Days)	c_3	$\mathcal{R}_c$
1	0–30	$8.03*10^3$	11.70
2	30–60	$1.29*10^4$	6.84
3	60–90	$1.59*10^4$	3.82
4	90–120	$1.80*10^4$	1.81
5	120–150	$1.94*10^4$	0.35

Regarding I, H, and the total number of deaths, during the first few days, the vaccination strategies do not make a big difference. At the end, the vaccinations drive the mentioned subpopulations to zero, and consequently, the number of cumulative deaths is stabilized, since $\mathcal{R}_c \leq 1$; see Table 5. Without vaccination $\mathcal{R}_c > 1$, hence the increase of the total number of deaths observed during the last period.

With the chosen c_1 and c_3 values, $v(t)$ follows the desired behavior; when there is a vaccine delivery, there is an increment in vaccinations and thereafter it tends to c_3/c_1. An increase of c_2 can modify this tendency when there is a rise in the number of hospitalized people; during the time period 0–30 days, when $c_2 = 0.05$, the number of vaccinations continuous growing instead of drifting to a constant value. With respect to $v_s(t)$, at

the beginning of each time period, the stock is greater than in the previous one (i.e., $v_s((n-1)T) < v_s(nT)$), since not all the vaccines are being implemented.

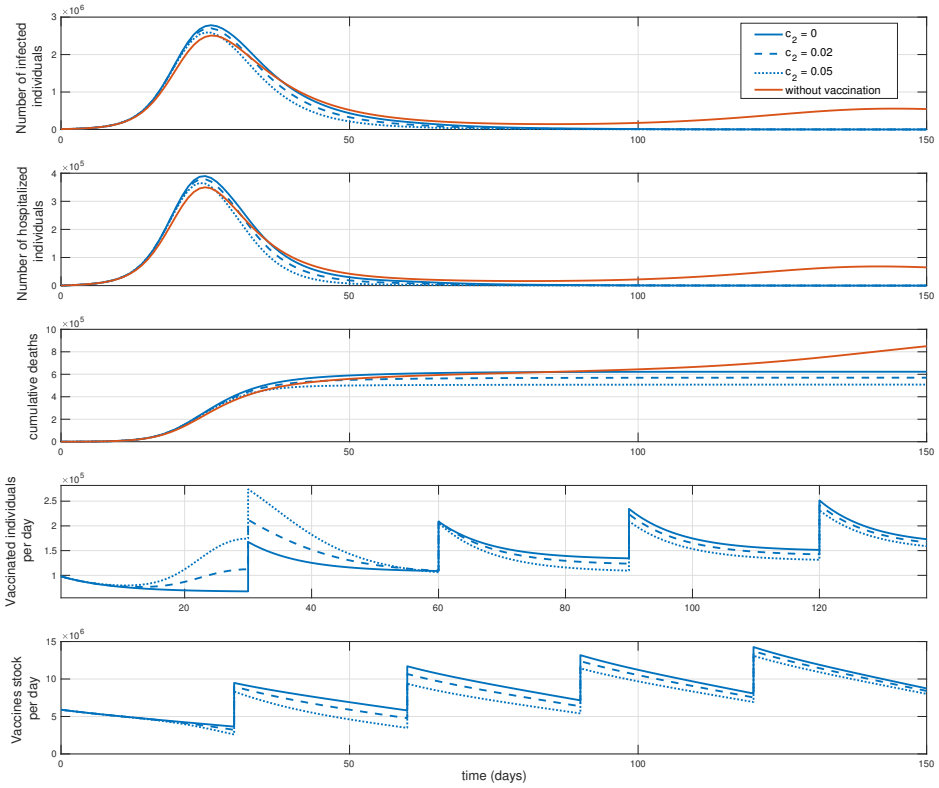

Figure 8. Evolution of infected (I) and H, cumulative deaths, v, and vaccines stock (v_s) with respect to time, with the initial conditions $S(0) = 7.42 * 10^6$, $I(0) = 1000$, $H(0) = 50$, $R(0) = 40 * 10^6$, and $v(0) = 0$. The blue lines simulate the cases in which a vaccination strategy is implemented, whereas the red lines show the behavior when there is no vaccination.

5. Discussion

An epidemic model consisting of susceptibles, non-seriously infected, hospitalized, and recovered subpopulations (SIHR) has been built up. In addition, a vaccination policy has also been included where the vaccination and hospitalization state variables are fed back and controlled with the tuning parameters c_1 and c_2, respectively. For more design freedom, another parameter (c_3) and a time-varying function ($f(t)$) have been added. This vaccination design is advantageous, since data regarding hospitalized people and vaccinated individuals are usually known.

The positivity of the model without vaccination has been proved. Considering the model with vaccination, a very impulsive one could provoke the negativeness of either the susceptible subpopulation or the vaccination stock. Therefore, in Theorem 2, the mentioned characteristic is taken into account, and the positivity of this model is proved under certain conditions. Then, P_{df} and P_{ee} as well as the conditions for their existence have been obtained. From the analysis of the local asymptotic stability of P_{df}, the analytical expression for $\mathcal{R}_c$ has been calculated, which gives broad information; when $\mathcal{R}_c < 1$, in addition to P_{df} being locally asymptotically stable, P_{ee} is not reachable. Contrary, when $\mathcal{R}_c > 1$, P_{df} is not locally asymptotically stable and P_{ee} is reachable. In addition, considering that the vaccination tuning parameters are constant with respect to time, the expression for β_c, so the local asymptotic stability of P_{df} is ensured, has been calculated. P_{df} has been proved to be globally stable when β is below β_c. The local asymptotic stability of P_{ee} has also been proved; when a vaccination is being applied, the stability is conditioned by some constrains, whereas the model without vaccines is not.

To study how the COVID-19 epidemic might evolve under different initial conditions, vaccination strategies, or average contact rate, data concerning population such as the natural death rate, birth rates, etc. have been gathered from official sources, and some features regarding COVID-19 disease (i.e., transmission probability) have also been collected. Firstly, an outbreak has been simulated when the conditions for the global stability are met, and even if a good result regarding the total number of deaths is attained, the number of contact rates needed for that purpose (approximately an average of 0.66 contacts per day) is very low and not affordable from a real point of view. Then, two simulations have been carried out to study the implications of the local asymptotic stability/instability; with a slight difference in vaccination and the same contact rates, during the first days, the differences between both is not prominent. However, after some time, one reaches P_{df} while the other reaches P_{ee}, which implies that the deaths stop and continue constantly, respectively. Therefore, it is concluded that from the public health point of view, governments should always try to maintain $\mathcal{R}_c < 1$, since by increasing the total vaccines administration 1.3% (from $82.10 * 10^6$ to $113.75 * 10^6$ in two years), the total number of deaths during that time decreases approximately four times (from $2.35 * 10^6$ to $509.22 * 10^3$).

Regarding the stability of the endemic equilibrium point, two cases have been considered: P_{ee}^{nv} and P_{ee}. In the first particular case, the stability is conditioned by the positivity of two terms (the equilibrium point is locally asymptotically stable when both terms are positive) derived from the Routh–Hurwitz criterion, which has been proved to be positive if P_{ee}^{nv} is reachable. When vaccines are being implemented, from Rouche's theorem, it has been concluded that it is sufficient if c_2 fulfills two conditions to ensure the local asymptotic stability of P_{ee}. In both cases, numerical simulations have been carried out with a regular vaccination, and it has been found that both cases match with the theoretical results.

The response of the hospitalized subpopulation with respect to different vaccination functions (constant, proportional, and state feedback) has been simulated, and the results have been compared; with the state feedback vaccination, its behavior can be easily adapted to a desired performance (e.g., a vaccination without peaks).

The last simulation could stand for a real-case example; a vaccines delivery function ($v_d(t)$) and vaccines stock function ($v_s(t)$) have been included, and c_1, c_3, and $f(t)$ have been chosen to match a vaccine specification; that is, $f(t)$ has been chosen as a periodic pulse-type function, so an impulsive vaccination is obtained, and the selected c_1 and c_3 drive vaccination to a desired steady value after a while. Several simulations have been carried out for different c_2 values, and the results have been compared with the case in which no vaccination is applied. When vaccines are implemented, the infected subpopulation tends to zero, and consequently the number of deaths do, too. With greater values of c_2, better results are shown since the number of vaccinated individuals at the beginning increases. For instance, the last simulation shows that with a periodic vaccines delivery, it is possible to eradicate the disease without administrating all the doses (i.e., the vaccines stock increases with respect to time), which is very important in case future outbreaks are anticipated (i.e., fall and winter are characterized by the prevalence of outbreaks).

Overall, the epidemic model with vaccination has been proved to be coherent in the sense that its solution and the equilibrium points are non-negative under certain conditions. Moreover, from the global and local asymptotic stability analysis of P_{df}, the conditions that force the disappearance of the disease have been obtained. With the Routh–Hurwitz criterion, the conditions for the local asymptotic stability of P_{ee} have been also derived. Then, based on real data, numerical values have been assigned to the parameters, and different simulations have been carried out; it has been found that the conditions for P_{df} global stability are difficult to accomplish, whereas for the local asymptotic stability, they are quite affordable. In the last simulation, it has been demonstrated that the implemented vaccination, as a result of the way in which it is built up and its free-design parameters and time-dependent function, can be easily adapted to desired requirements.

Taking into account that usually the death rate differs notoriously between age groups, our future work will consider this model as the baseline for an age-group epidemic model.

Then, the optimal control problem can be formulated, where the performance measure could be defined to follow the minimum control effort (i.e., least waste of resources), to transfer a system from an arbitrary initial state to the target state (the P_{df}) in minimum time and to maximize the deviation of the hospitalized subpopulation state from the hospital's bed limit.

Author Contributions: Conceptualization, C.L., M.D.l.S. and S.A.-Q.; methodology, C.L. and S.A.-Q.; software, C.L.; validation, S.A.-Q.; formal analysis, C.L., M.D.l.S. and S.A.-Q.; investigation, C.L., M.D.l.S. and S.A.-Q.; resources, C.L.; data curation, C.L.; writing—original draft preparation, C.L.; writing—review and editing, S.A.-Q.; visualization, C.L.; supervision, M.D.l.S.; project administration, M.D.l.S.; funding acquisition, M.D.l.S. All authors have read and agreed to the published version of the manuscript.

Funding: This research received support from the Basque Government through grant IT1555-22.

Data Availability Statement: The data presented in this study are available in the article and references.

Acknowledgments: The authors are grateful to the Basque Government for its support through the grant for Grant IT1555-22.

Conflicts of Interest: The authors declare no conflicts of interest. The funders had no role in the design of the study; in the collection, analyses, or interpretation of data; in the writing of the manuscript; or in the decision to publish the results.

Abbreviations

The following abbreviations are used in this manuscript:

S	Susceptible subpopulation
I	Non-seriously infected subpopulation
H	Hospitalized subpopulation
R	Recovered subpopulation
P_{df}	Disease-free equilibrium point
P_{df}^{nv}	Disease-free equilibrium point in absence of vaccination
P_{ee}	Enedemic equilibrium point
P_{ee}^{nv}	Endemic equilibrium point in absence of vaccination
$\mathcal{R}_0$	Basic reproduction number
$\mathcal{R}_c$	Controlled reproduction number
SARS-CoV	Severe acute respiratory syndrome coronavirus
WHO	World Health Organization

Appendix A. Proof of Theorem 4 (Vaccination Free Case)

To obtain the condition for which the endemic equilibrium point is locally asymptotically stable, the previously calculated Jacobian matrix, see (57), has been considered but without vaccination (i.e., $c_1 = c_2 = c_3 = f = 0$). Therefore, the expression (57) is reduced to

$$\mathbf{J} = \begin{pmatrix} -\beta i_{ee}^{nv}(1-s_{ee}^{nv}) - \mu & -\beta s_{ee}^{nv}(1-i_{ee}^{nv}) & \beta i_{ee}^{nv} s_{ee}^{nv} & \beta i_{ee}^{nv} s_{ee}^{nv} + \rho \\ k_4 i_{ee}^{nv}(1-s_{ee}^{nv}) & k_4 s_{ee}^{nv}(1-i_{ee}^{nv}) & -k_4 i_{ee}^{nv} s_{ee}^{nv} - k_1 & -k_4 i_{ee}^{nv} s_{ee}^{nv} \\ \beta p i_{ee}^{nv}(1-s_{ee}^{nv}) & \beta p s_{ee}^{nv}(1-i_{ee}^{nv}) & -\beta p i_{ee}^{nv} s_{ee}^{nv} - k_2 & -\beta p i_{ee}^{nv} s_{ee}^{nv} \\ 0 & \gamma_1 & \gamma_2 & -k_3 \end{pmatrix}, \tag{A1}$$

where

$$\begin{aligned} s_{ee}^{nv} &= s_{ee} = \tfrac{S_{ee}}{N_{ee}} = \tfrac{k_1}{k_4} = \tfrac{1}{\mathcal{R}_0}, \quad \text{and} \\ i_{ee}^{nv} &= \tfrac{I_{ee}^{nv}}{N_{ee}^{nv}} = \tfrac{\mu k_2 (1-p) H_{ee}^{nv}}{k_1 p (\Lambda - \alpha H_{ee}^{nv})} = \tfrac{k_2 k_3 (1-p)\mu(\mathcal{R}_0 - 1)}{\mathcal{R}_0\{k_1 k_2 \mu + \rho[p\gamma_1(\alpha+\mu) + (1-p)\gamma_2\mu + \mu(\alpha+\mu)] - k_1 k_3 p\alpha\}}. \end{aligned} \tag{A2}$$

Taking into account Proposition 3, the normalized subpopulations will be positive and bounded; that is, $0 < s_{ee}^{nv} < 1$ and $0 < i_{ee}^{nv} < 1$.

Let us solve the eigenvalue problem $|\mathbf{J} - \lambda \mathbb{I}_{4x4}| = 0$, that is:

$$\left| \begin{pmatrix} -\beta i_{ee}^{nv}(1-s_{ee}^{nv}) - \mu - \lambda & -\beta s_{ee}^{nv}(1-i_{ee}^{nv}) & \beta i_{ee}^{nv} s_{ee}^{nv} & \beta i_{ee}^{nv} s_{ee}^{nv} + \rho \\ k_4 i_{ee}^{nv}(1-s_{ee}^{nv}) & k_4 s_{ee}^{nv}(1-i_{ee}^{nv}) - k_1 - \lambda & -k_4 i_{ee}^{nv} s_{ee}^{nv} - k_1 & -k_4 i_{ee}^{nv} s_{ee}^{nv} \\ \beta p i_{ee}^{nv}(1-s_{ee}^{nv}) & \beta p s_{ee}^{nv}(1-i_{ee}^{nv}) & -\beta p i_{ee}^{nv} s_{ee}^{nv} - k_2 - \lambda & -\beta p i_{ee}^{nv} s_{ee}^{nv} \\ 0 & \gamma_1 & \gamma_2 & -k_3 - \lambda \end{pmatrix} \right| = 0, \tag{A3}$$

and by direct calculations, it is obtained that:

$$\lambda^4 + a_3^{nv}\lambda^3 + a_2^{nv}\lambda^2 + a_1^{nv}\lambda + a_0^{nv} = 0 \tag{A4}$$

where

$$\begin{array}{l} a_3^{nv} = \beta i_{ee}^{nv} b_3 + k_2 + k_3 + \mu > 0, \\ a_2^{nv} = \beta i_{ee}^{nv} b_2 + \mu(k_3 + k_2) + k_2 k_3 > 0, \\ a_1^{nv} = \beta i_{ee}^{nv} b_1 + \mu k_2 k_3 > 0, \quad \text{and} \\ a_0^{nv} = \beta i_{ee}^{nv} b_0 > 0, \end{array} \tag{A5}$$

and

$$\begin{array}{l} b_3 = 1, \\ b_2 = k_1 + k_2 + k_3 - \alpha p s_{ee}^{nv}, \\ b_1 = (k_1 + k_3)(1 - p s_{ee}^{nv})\alpha + [p\gamma_1 + (1-p)\gamma_2 + 2\mu]\rho + (k_1 + \mu)(\gamma_2 + \mu) + k_1\mu, \quad \text{and} \\ b_0 = (k_1 + \rho)(1 - p s_{ee}^{nv})\alpha\mu + p(1 - s_{ee}^{nv})\gamma_1\alpha\rho + (1-p)\gamma_2\rho\mu + [k_1\gamma_2 + (p\rho + \mu)\gamma_1 + k_3\mu]\mu. \end{array} \tag{A6}$$

The Routh table is formed by the following terms:

$$\begin{array}{l} d_1^{nv} = -\dfrac{\begin{vmatrix} 1 & a_2^{nv} \\ a_3^{nv} & a_1^{nv} \end{vmatrix}}{a_3^{nv}} = \dfrac{-a_1^{nv} + a_3^{nv} a_2^{nv}}{a_3^{nv}}, \\ d_2^{nv} = -\dfrac{\begin{vmatrix} 1 & a_0^{nv} \\ a_3^{nv} & 0 \end{vmatrix}}{a_3^{nv}} = a_0^{nv}, \quad \text{and} \\ g_1^{nv} = -\dfrac{\begin{vmatrix} a_3^{nv} & a_1^{nv} \\ d_1^{nv} & d_2^{nv} \end{vmatrix}}{d_1^{nv}} = \dfrac{-a_3^{nv} d_2^{nv} + d_1^{nv} a_1^{nv}}{d_1^{nv}} = \dfrac{-a_3^{nv} a_0^{nv} + d_1^{nv} a_1^{nv}}{d_1^{nv}}. \end{array} \tag{A7}$$

Considering that the endemic equilibrium point is reachable ($0 < i_{ee}^{nv} < 1$ and $0 < s_{ee}^{nv} < 1$), and that the parameters are non-negative (they fulfill the condition given in (1)), it follows that d_1^{nv} and g_1^{nv} are positive. Therefore, from the Routh–Hurwitz criterion, it is concluded that the polynomial (A4) has its roots on the open left-half plane, and consequently, the endemic equilibrium point without vaccination is locally asymptotically stable.

Appendix B. Proof of Theorem 5 (Vaccination Control)

Considering the expression for N_{ee} in (37), the normalized subpopulations s_{ee} and i_{ee} are calculated:

$$\begin{array}{l} s_{ee} = \dfrac{S_{ee}}{N_{ee}} = \dfrac{k_1}{k_4} = \dfrac{1}{\mathcal{R}_0} \quad \text{and} \\ i_{ee} = \dfrac{I_{ee}}{N_{ee}} = \dfrac{\mu k_2 (1-p) H_{ee}}{k_1 p (\Lambda - \alpha H_{ee})} = \dfrac{n_i}{d_{i1} + c_2 d_{i2}}, \end{array} \tag{A8}$$

where

$$\begin{array}{l} n_i = k_2 k_3 (1-p)\mu(\mathcal{R}_c - 1), \\ d_{i1} = \mathcal{R}_0\{k_1 k_2 \mu + \rho[p\gamma_1(\alpha + \mu) + (1-p)\gamma_2\mu + \mu(\alpha + \mu)] - k_1 k_3 p \alpha \dfrac{\mathcal{R}_c}{\mathcal{R}_0}\} \quad \text{and} \\ d_{i2} = \dfrac{\mathcal{R}_0 k_1 p \mu}{c_1}. \end{array} \tag{A9}$$

Each normalized subpopulation will be positive if the conditions given in Proposition 3 are fulfilled, and they will be bounded ($0 < s_{ee} < 1$ and $0 < i_{ee} < 1$) since N_{ee} is the sum of all subpopulations.

To analyze the local stability of the endemic equilibrium point, let us take the previously calculated Jacobian matrix, see (57), and evaluate it above P_{ee}; see terms in (36), (37) and (A8):

$$\mathbf{J} = \begin{pmatrix} -\beta i_{ee}(1-s_{ee}) - \mu & -\beta s_{ee}(1-i_{ee}) & \beta i_{ee}^{nv} s_{ee}^{nv} & \beta i_{ee}^{nv} s_{ee}^{nv} + \rho & -1 \\ k_4 i_{ee}(1-s_{ee}) & k_4 s_{ee}(1-i_{ee}) - k_1 & -k_4 i_{ee}^{nv} s_{ee}^{nv} - k_1 & -k_4 i_{ee}^{nv} s_{ee}^{nv} & 0 \\ \beta p i_{ee}(1-s_{ee}) & \beta p s_{ee}(1-i_{ee}) & -\beta p i_{ee}^{nv} s_{ee}^{nv} - k_2 & -\beta p i_{ee}^{nv} s_{ee}^{nv} & 0 \\ 0 & \gamma_1 & \gamma_2 & -k_3 & 1 \\ 0 & 0 & c_2 & 0 & -c_1 \end{pmatrix}, \tag{A10}$$

and the eigenvalues are obtained from the solution of the equation $|\mathbf{J} - \lambda \mathbb{I}_{5x5}| = 0$, that is:

$$\left| \begin{pmatrix} -\beta i_{ee}(1-s_{ee}) - \mu - \lambda & -\beta s_{ee}(1-i_{ee}) & \beta i_{ee}^{nv} s_{ee}^{nv} & \beta i_{ee}^{nv} s_{ee}^{nv} + \rho & -1 \\ k_4 i_{ee}(1-s_{ee}) & k_4 s_{ee}(1-i_{ee}) - \lambda & -k_4 i_{ee}^{nv} s_{ee}^{nv} - k_1 & -k_4 i_{ee}^{nv} s_{ee}^{nv} & 0 \\ \beta p i_{ee}(1-s_{ee}) & \beta p s_{ee}(1-i_{ee}) & -\beta p i_{ee}^{nv} s_{ee}^{nv} - k_2 - \lambda & -\beta p i_{ee}^{nv} s_{ee}^{nv} & 0 \\ 0 & \gamma_1 & \gamma_2 & -k_3 - \lambda & 1 \\ 0 & 0 & c_2 & 0 & -c_1 - \lambda \end{pmatrix} \right| = 0, \tag{A11}$$

which leads to

$$\lambda^5 + a_4' \lambda^4 + a_3' \lambda^3 + a_2' \lambda^2 + a_1' \lambda + a_0 = 0, \tag{A12}$$

where

$$\begin{aligned} a_4' &= a_3^v + c_1, \\ a_3' &= a_2^v + c_1 a_3^v, \\ a_2' &= a_1^v + c_1 a_2^v + \delta, \\ a_1' &= a_0^v + c_1 a_1^v + (k_1 + \mu)\delta, \quad \text{and} \\ a_0' &= c_1 a_0^v + k_1 \mu \delta, \end{aligned} \tag{A13}$$

and

$$\begin{aligned} a_3^v &= \beta i_{ee} b_3 + k_2 + k_3 + \mu > 0, \\ a_2^v &= \beta i_{ee} b_2 + \mu(k_3 + k_2) + k_2 k_3 > 0, \\ a_1^v &= \beta i_{ee} b_1 + \mu k_2 k_3 > 0, \\ a_0^v &= \beta i_{ee} b_0 > 0, \quad \text{and} \\ \delta &= c_2 p \beta i_{ee}. \end{aligned} \tag{A14}$$

Note that the parameter a_i^v, where $i = 0, 1, 2, 3$, is related to the coefficients of the polynomial (A4) defined in Appendix A; that is, taking into account the expression for a_i^v in (A14), if one substitutes i_{ee} for i_{ee}^{nv}, then a_i^{nv} is obtained. One can rewrite (A12) as follows:

$$(\lambda^4 + a_3^v \lambda^3 + a_2^v \lambda^2 + a_1^v \lambda + a_0^v)(\lambda + c_1) + \delta(\lambda^2 + (k_1 + \mu)\lambda + k_1 \mu) = 0. \tag{A15}$$

Considering that $i_{ee} = \frac{n_i}{d_{i1} + c_2 d_{i2}}$, then the expression above can be rewritten as:

$$\begin{aligned} &d_{i1}(\lambda^4 + a_3 \lambda^3 + a_2 \lambda^2 + a_1 \lambda + a_0)(\lambda + c_1) \\ &+(\lambda + \mu)\left[\tfrac{c_2}{c_1} d_{i2}(\lambda + k_3)(\lambda + k_2)(\lambda + c_1)\lambda + c_2 p \beta n_i(\lambda + k_1)\right] = 0, \end{aligned} \tag{A16}$$

where a_i is equal to a_i^v, see expression (A14), but considering $i_{ee} = \frac{n_i}{d_{i1}}$ instead of $i_{ee} = \frac{n_i}{d_{i1} + c_2 d_{i2}}$.

Let D be a bounded domain and ∂D be its boundary. Let $F(\lambda) = f(\lambda) + \Delta f(\lambda)$, where $f(\lambda)$ and $\Delta f(\lambda)$ are analytical on $D \cup \partial D$. If $|f(\lambda)| > |\Delta f(\lambda)|$ for $\lambda \in \partial D$, by Rouche's theorem [47], $f(\lambda)$ and $F(\lambda)$ have the same number of roots in D. Therefore, let us consider

$$\begin{aligned} f(\lambda) &= d_{i1}(\lambda^4 + a_3 \lambda^3 + a_2 \lambda^2 + a_1 \lambda + a_0)(\lambda + c_1) \quad \text{and} \\ \Delta f(\lambda) &= (\lambda + \mu)\left[\tfrac{d_{i2}}{c_1}(\lambda + k_3)(\lambda + k_2)(\lambda + c_1)\lambda + p \beta n_i(\lambda + k_1)\right], \end{aligned} \tag{A17}$$

and hence, the polynomial (A16) can be rewritten as

$$F(\lambda) = f(\lambda) + c_2 \Delta f(\lambda). \tag{A18}$$

The roots of $\lambda^4 + a_3^{nv}\lambda^3 + a_2^{nv}\lambda^2 + a_1^{nv}\lambda + a_0^{nv}$ had a negative real part (all roots are inside the closed left-half plane) as far as $0 < i_{ee}^{nv} < 1$ and $0 < s_{ee} < 1$, see the proof of Theorem 5 in Appendix A, and consequently, $f(\lambda)$ roots will also be inside the closed left-half plane since $\frac{n_i}{d_1}$ fulfills the condition $0 < \frac{n_i}{d_1} < 1$. Let D correspond to the closed right-half plane and $\partial D = \partial D_1 \cup \partial D_2$ to its boundary, where $\partial D_1 = \{|\lambda| = R : \Re(\lambda) > 0\}$ and $\partial D_2 = \{\lambda = i\omega : |\lambda| < R\}$. Since $f(\lambda)$ and $\Delta f(\lambda)$ are polynomials, it is straightforward that they are analytical on $D \cup \partial D$. If $|f(\lambda)| > c_2|\Delta f(\lambda)|$ for $\lambda \in \partial D$, from Rouche's theorem, it follows that $F(\lambda)$ roots are inside the open left-half plane.

Considering the boundary ∂D_1, if

$$c_2 < \frac{c_1 d_{i1}}{\mathcal{R}_0 k_1 p \mu} = \frac{c_1\{k_1 k_2 \mu + \rho[p\gamma_1(\alpha+\mu) + (1-p)\gamma_2\mu + \mu(\alpha+\mu)] - k_1 k_3 p\alpha \frac{\mathcal{R}_c}{\mathcal{R}_0}\}}{k_1 p \mu}, \tag{A19}$$

then $|f(\lambda)| > c_2|\Delta f(\lambda)|$ for all $\lambda \in \partial D_1$ as $R \to \infty$. Regarding ∂D_2, one finds that the following condition must be fulfilled:

$$\sup_{\omega \in \mathbb{R}} |G(i\omega)| = c_2 \sup_{\omega \in \mathbb{R}} \left(\frac{|\Delta f(i\omega)|}{|f(i\omega)|} \right) < 1, \tag{A20}$$

and considering its symmetry, it follows that

$$\sup_{\omega \in \mathbb{R}_+} |G(i\omega)| = c_2 \sup_{\omega \in \mathbb{R}_+} \left(\frac{|\Delta f(i\omega)|}{|f(i\omega)|} \right) < 1, \tag{A21}$$

where $\mathbb{R}_+ = \{x \in \mathbb{R} : x \geq 0\}$.

References

1. Wu, F.; Zhao, S.; Yu, B.; Chen, Y.M.; Wang, W.; Song, Z.G.; Zhang, Y.Z. A new coronavirus associated with human respiratory disease in China. *Nature* **2020**, *579*, 265–269. [CrossRef]
2. Zhou, P.; Yang, X.L.; Wang, X.G.; Hu, B.; Zhang, L.; Zhang, W.; Shi, Z.L. A pneumonia outbreak associated with a new coronavirus of probable bat origin. *Nature* **2020**, *579*, 270–273. [CrossRef]
3. Tao, Z.; Qunfu, W.; Zhigang, Z. Probable pangolin origin of SARS-CoV-2 associated with the COVID-19 outbreak. *Curr. Biol.* **2020**, *30*, 1346–1351.e2. [CrossRef]
4. Huang, C.; Wang, Y.; Li, X.; Ren, L.; Zhao, J.; Hu, Y.; Cao, B. Clinical features of patients infected with 2019 novel coronavirus in Wuhan, China. *Lancet* **2020**, *395*, 497–506. [CrossRef]
5. Deng, Y.; Liu, W.; Liu, K.; Fang, Y.Y.; Shang, J.; Zhou, L.; Liu, H.G. Clinical characteristics of fatal and recovered cases of coronavirus disease 2019 in Wuhan, China: A retrospective study. *Chin. Med. J.* **2020**, *133*, 1261–1267. [CrossRef] [PubMed]
6. World Health Organization. WHO Director-General's Opening Remarks at the Media Briefing on COVID-19—11 March 2020. Available online: https://www.who.int/director-general/speeches/detail/who-director-general-s-opening-remarks-at-the-media-briefing-on-covid-19---11-march-2020 (accessed on 28 July 2023).
7. Keeling, M.J.; Rohani, P. *Modeling Infectious Diseases in Humans and Animals*; Princeton University Press: Princeton, NJ, USA, 2008.
8. Brauer, F.; van den Driessche, P.; Wu, J. *Mathematical Epidemiology*, 1st ed.; Springer: Berlin/Heidelberg, Germany, 2008.
9. Kermack, W.O.; McKendrick, A.G.; Walker, G.T. A contribution to the mathematical theory of epidemics. *Proc. R. Soc. Lond. Ser. A Contain. Pap. Math. Phys. Character* **1927**, *115*, 700–721. [CrossRef]
10. Martcheva, M. The SIR Model with Demography: General Properties of Planar Systems. In *An Introduction to Mathematical Epidemiology*; Springer: Boston, MA, USA, 2015; pp. 33–66. [CrossRef]
11. Hethcote, H.W. The Mathematics of Infectious Diseases. *SIAM Rev.* **2000**, *42*, 599–653. [CrossRef]
12. Ma, J.; Ma, Z. Epidemic threshold conditions for seasonally forced SEIR models. *Math. Biosci. Eng.* **2006**, *3*, 161–172. [CrossRef]
13. Li, M.Y.; Muldowney, J.S. Global stability for the SEIR model in epidemiology. *Math. Biosci.* **1995**, *125*, 155–164. [CrossRef]
14. Ahmad, W.; Rafiq, M.; Abbas, M. Mathematical analysis to control the spread of Ebola virus epidemic through voluntary vaccination. *Eur. Phys. J. Plus* **2020**, *135*, 775. [CrossRef]
15. Wodajo, F.A.; Mekonnen, T.T. Effect of Intervention of Vaccination and Treatment on the Transmission Dynamics of HBV Disease: A Mathematical Model Analysis. *J. Math.* **2022**, *2022*, 9968832. [CrossRef]

16. Wei, F.; Zhou, R.; Jin, Z.; Huang, S.; Peng, Z.; Wang, J.; Xu, X.; Zhang, X.; Xu, J.; Bai, Y.; et al. COVID-19 transmission driven by age-group mathematical model in Shijiazhuang City of China. *Infect. Dis. Model.* **2023**, *8*, 1050–1062. [CrossRef] [PubMed]
17. Zhou, L.; Wang, Y.; Xiao, Y.; Li, M.Y. Global dynamics of a discrete age-structured SIR epidemic model with applications to measles vaccination strategies. *Math. Biosci.* **2019**, *308*, 27–37. [CrossRef]
18. Inaba, H. Threshold and stability results for an age-structured epidemic model. *J. Math. Biol.* **1990**, *28*, 411–434. [CrossRef] [PubMed]
19. Bi, K.; Chen, Y.; Zhao, S.; Ben-Arieh, D.; Wu, C.H. A new zoonotic visceral leishmaniasis dynamic transmission model with age-structure. *Chaos Solitons Fractals* **2020**, *133*, 109622. [CrossRef]
20. Stone, L.; Shulgin, B.; Agur, Z. Theoretical examination of the pulse vaccination policy in the SIR epidemic model. *Math. Comput. Model.* **2000**, *31*, 207–215. [CrossRef]
21. Shulgin, B.; Stone, L.; Agur, Z. Pulse vaccination strategy in the SIR epidemic model. *Bull. Math. Biol.* **1998**, *60*, 1123–1148. [CrossRef] [PubMed]
22. Liu, X.; Takeuchi, Y.; Iwami, S. SVIR epidemic models with vaccination strategies. *J. Theor. Biol.* **2008**, *253*, 1–11. [CrossRef]
23. Lu, Z.; Chi, X.; Chen, L. The effect of constant and pulse vaccination on SIR epidemic model with horizontal and vertical transmission. *Math. Comput. Model.* **2002**, *36*, 1039–1057. [CrossRef]
24. Hwang, Y.G.; Kwon, H.D.; Lee, J. Feedback control problem of an SIR epidemic model based on the Hamilton-Jacobi-Bellman equation. *Math. Biosci. Eng.* **2020**, *17*, 2284–2301. [CrossRef]
25. Bilal, M.; Ahmad, I.; Babar, S.A.; Shahzad, K. State Feedback and Synergetic controllers for tuberculosis in infected population. *IET Syst. Biol.* **2021**, *15*, 83–92. [CrossRef] [PubMed]
26. Li, Z.; Hong, J.; Kim, J.; Yu, C. Control Design and Stability Analysis of a Two-Infectious-State Awareness Epidemic Model. In Proceedings of the 2019 12th Asian Control Conference (ASCC), Kitakyushu, Japan, 9–12 June 2019; pp. 704–709.
27. She, B.; Sundaram, S.; Paré, P.E. A Learning-Based Model Predictive Control Framework for Real-Time SIR Epidemic Mitigation. In Proceedings of the 2022 American Control Conference (ACC), Atlanta, GA, USA, 8–10 June 2022; pp. 2565–2570. [CrossRef]
28. Bi, K.; Chen, Y.; Wu, C.H.J.; Ben-Arieh, D. Learning-based impulse control with event-triggered conditions for an epidemic dynamic system. *Commun. Nonlinear Sci. Numer. Simul.* **2022**, *108*, 106204. [CrossRef]
29. Zugarini, A.; Meloni, E.; Betti, A.; Panizza, A.; Corneli, M.; Gori, M. An Optimal Control Approach to Learning in SIDARTHE Epidemic model. *arXiv* **2020**, arXiv:2010.14878.
30. Yin, S.; Wu, J.; Song, P. Optimal control by deep learning techniques and its applications on epidemic models. *J. Math. Biol.* **2023**, *86*, 36. [CrossRef]
31. Demertzis, K.; Taketzis, D.; Tsiotas, D.; Magafas, L.; Iliadis, L.; Kikiras, P. Pandemic Analytics by Advanced Machine Learning for Improved Decision Making of COVID-19 Crisis. *Processes* **2021**, *9*, 1267. [CrossRef]
32. Youssef, H.M.; Alghamdi, N.; Ezzat, M.A.; El-Bary, A.A.; Shawky, A.M. A proposed modified SEIQR epidemic model to analyze the COVID-19 spreading in Saudi Arabia. *Alex. Eng. J.* **2022**, *61*, 2456–2470. [CrossRef]
33. Ghosh, J.K.; Biswas, S.K.; Sarkar, S.; Ghosh, U. Mathematical modelling of COVID-19: A case study of Italy. *Math. Comput. Simul.* **2022**, *194*, 1–18. [CrossRef] [PubMed]
34. Chen, M.; Li, M.; Hao, Y.; Liu, Z.; Hu, L.; Wang, L. The introduction of population migration to SEIAR for COVID-19 epidemic modeling with an efficient intervention strategy. *Inf. Fusion* **2020**, *64*, 252–258. [CrossRef]
35. Saha, S.; Samanta, G.P.; Nieto, J.J. Epidemic model of COVID-19 outbreak by inducing behavioural response in population. *Nonlinear Dyn.* **2020**, *102*, 455–487. [CrossRef]
36. Etxeberria-Etxaniz, M.; Alonso-Quesada, S.; De la Sen, M. On an SEIR Epidemic Model with Vaccination of Newborns and Periodic Impulsive Vaccination with Eventual On-Line Adapted Vaccination Strategies to the Varying Levels of the Susceptible Subpopulation. *Appl. Sci.* **2020**, *10*, 8296. [CrossRef]
37. Ottaviano, S.; Sensi, M.; Sottile, S. Global stability of SAIRS epidemic models. *Nonlinear Anal. Real World Appl.* **2022**, *65*, 103501. [CrossRef]
38. Diagne, M.L.; Rwezaura, H.; Tchoumi, S.Y.; Tchuenche, J.M. A Mathematical Model of COVID-19 with Vaccination and Treatment. *Comput. Math. Methods Med.* **2021**, *2021*, 1250129. [CrossRef]
39. Alonso-Quesada, S.; De la Sen, M.; Nistal, R. An SIRS Epidemic Model Supervised by a Control System for Vaccination and Treatment Actions Which Involve First-Order Dynamics and Vaccination of Newborns. *Mathematics* **2022**, *10*, 36. [CrossRef]
40. INE. Indicadores Demográficos báSicos [Database]. 2019. Available online: https://www.ine.es/dyngs/INEbase/operacion.htm?c=Estadistica_C&cid=1254736177003&menu=resultados&secc=1254736195380&idp=1254735573002#!tabs-1254736195380 (accessed on 20 October 2023).
41. Mousa, A.; Winskill, P.; Watson, O.J.; Ratmann, O.; Monod, M.; Ajelli, M.; Whittaker, C. Social contact patterns and implications for infectious disease transmission—A systematic review and meta-analysis of contact surveys. *eLife* **2021**, *10*, 70294. [CrossRef] [PubMed]
42. Thompson, H.A.; Mousa, A.; Dighe, A.; Fu, H.; Arnedo-Pena, A.; Barrett, P.; Ferguson, N.M. Severe acute respiratory syndrome coronavirus 2 (SARS-CoV-2) setting-specific transmission rates: A systematic review and meta-analysis. *Clin. Infect. Dis.* **2021**, *73*, 754–764. [CrossRef] [PubMed]
43. Thomas, B.; Neves, A.L.; Alboksmaty, A.; Ashrafian, H.; Flott, K.; Fowler, A.; Clarke, J. Trends and associated factors for Covid-19 hospitalisation and fatality risk in 2.3 million adults in England. *Nat. Commun.* **2022**, *13*, 2356. [CrossRef]

44. Christel, F.; Steven, A.; Dominique, V.B.; Geert, M.; Erika, V.; Niel, H. Time between Symptom Onset, Hospitalisation and Recovery or Death: Statistical Analysis of Belgian COVID-19 Patients. *Int. J. Environ. Res. Public Health* **2020**, *17*, 7560. [CrossRef]
45. Addo, I.Y.; Dadzie, F.A.; Okeke, S.R.; Boadi, C.; Boadu, E.F. Duration of immunity following full vaccination against SARS-CoV-2: A systematic review. *Arch. Public Health* **2022**, *80*, 200. [CrossRef]
46. Vidyasagar, M. *Nonlinear Systems Analysis*, 2nd ed.; Prentice-Hall, Inc.: Upper Saddle River, NJ, USA, 1993.
47. Gamelin, T. *Complex Analysis*; Undergraduate texts in mathematicsp; Springer: Berlin/Heidelberg, Germany, 2001.
48. De la Sen, M.; Nistal, R.; Alonso-Quesada, S.; Ibeas, A. Some Formal Results on Positivity, Stability, and Endemic Steady-State Attainability Based on Linear Algebraic Tools for a Class of Epidemic Models with Eventual Incommensurate Delays. *Discret. Dyn. Nat. Soc.* **2019**, *2019*, 8959681. [CrossRef]
49. Zhang, L.; Zhu, J.; Wang, X.; Yang, J.; Liu, X.F.; Xu, X.K. Characterizing COVID-19 Transmission: Incubation Period, Reproduction Rate, and Multiple-Generation Spreading. *Front. Phys.* **2021**, *8*, 589963. [CrossRef]